Spring 1993

Robust Control of Nonlinear Multibody Flexible Space Structures

Atul G. Kelkar
Old Dominion University

ROBUST CONTROL OF NONLINEAR MULTIBODY FLEXIBLE SPACE STRUCTURES

ATUL G. KELKAR
MASTER OF SCIENCE, April 1990
Old Dominion University, Norfolk, VA 23529

A Thesis Submitted to the Faculty of
Old Dominion University in Partial Fulfillment of the
Requirements for the Degree of

DOCTOR OF PHILOSOPHY
ENGINEERING MECHANICS

OLD DOMINION UNIVERSITY
AUGUST 1993

Approved by:

Dr. Thomas E. Alberts (Director)	Dr. Suresh M. Joshi (Codirector)
Dr. Gene Hou	Dr. Oscar R. González
Dr. Jen K. Huang	

ABSTRACT

ROBUST CONTROL OF NONLINEAR MULTIBODY FLEXIBLE SPACE STRUCTURES

Atul G. Kelkar
Department of Mechanical Engineering and Mechanics
Old Dominion University
Director: Dr. Thomas E. Alberts
Co-Director: Dr. Suresh M. Joshi

A generic nonlinear math model of a multibody flexible system is developed. Asymptotic stability of such systems using dissipative compensators is established. It is proved that, under certain conditions, this class of systems exhibit global asymptotic stability under dissipative compensation. The dissipative compensators considered are static as well as dynamic dissipative compensators. The stability proofs are based on passivity approaches, Lyapunov methods, as well as a key property of such systems, i.e., skew-symmetricity of certain matrix. The importance of the stability results obtained is that the stability is robust to parametric uncertainties and modeling errors.

For static dissipative compensators, it is shown that stability is not only robust to parametric uncertainties and modeling errors but also to certain actuator and sensor nonlinearities. Actuator nonlinearities considered are $(0, \infty)$ sector

monotonically non-decreasing type, which include realistic nonlinearities such as the saturation nonlinearity. In the presence of dead-zone and hysteresis type nonlinearities, system trajectories do not approach equilibrium point asymptotically, however, it is shown that there is a compact region of ultimate boundedness and system trajectories do not go unbounded. The sensor nonlinearities considered are $(0, \infty)$ sector nonlinearities.

A more versatile class of dissipative compensators, called dynamic dissipative compensators, is next considered. A control designer has more design freedom with dynamic dissipative compensators than with the static dissipative type. The increased design degrees of freedom can be used to enhance the performance of the control system.

The synthesis techniques for static as well as dynamic dissipative compensators for multibody, nonlinear, flexible systems are currently unknown and it is a topic of future research. The asymptotic stability property of a static dissipative controller for multibody, nonlinear, flexible space structures is demonstrated through a simulation example. The example system used consists of a flexible 10-bay truss structure with a flexible, 2-link manipulator arm attached at one end of the truss. This example system is representative of the class of spacecraft envisioned for the future. missions. For dynamic dissipative compensators an application example is shown for a multibody planar system with an articulated member. The controller design is based on locally linearized models in the configuration space of the articulated member. This example also demonstrates the use of dissipative compensators in the integrated design framework.

ACKNOWLEDGEMENTS

I wish to express my appreciation to those who have been of great help in the preparation of this thesis. My advisor, Dr. Thomas E. Alberts, has been a very helpful committee chairman. My sincere thanks to him for his continued support and encouragement. I deeply appreciate his willingness to help and friendly nature. I wish to express my deep sense of gratitude to Dr. Suresh M. Joshi, committee co-chairman, for all his help throughout my research. It is his profound knowledge and expertise in the area of controls that made this research an enjoyable experience. His analytical ability, innovativeness and hard working nature will always inspire me. I am also greatful to Dr. Oscar Gonzales, Dr. Gene Hou and Dr. J-K. Huang for serving on my committee and for their valuable help in private consultations.

I would like to thank all members of the CSI-ADM team of NASA Langley Research Center for their guidance and technical support during my research work at NASA Langley. Also, the financial support from CSI-ADM team of NASA Langley Research Center is greatly acknowledged.

Finally, I would like to thank my family, to whom I owe a whole lot, for their continued moral support and understanding.

TABLE OF CONTENTS

LIST OF FIGURES

LIST OF TABLES

LIST OF SYMBOLS

r_P = position vector of point P in inertial frame

s_P = position vector of point P in its local body frame

R_P = undeformed position of point P in its local body frame

s_i = position vector of the origin of ith body frame in the central body frame

s_{i+1} = position vector of the origin of $(i+1)$th body frame in ith body frame

R_i = undeformed position of the origin of ith body frame in the central body frame

R_{i+1} = undeformed position of the origin of $(i+1)$th body frame in the ith body frame

${}^iA_{i+1}$ = rotational transformation matrix from ith frame to $(i+1)$th frame

E_K = total kinetic energy of the system

E_P = total potential energy of the system

L = Lagrangian of the system

$M(p)$ = mass-inertia matrix of the system

D = structural damping matrix of the system

K = stiffness matrix of the system

p = generalized coordinate

q = flexural coordinate

B = control influence matrix

V = Lyapunov function candidate

E = Modulus of elasticity

G_p = position gain matrix

G_r = rate gain matrix

μ = mass density

ρ = position vector in the local frame

ψ_p = position sensor nonlinearity

ψ_r = rate sensor nonlinearity

y_p = position output

y_r = rate output

Φ = stain energy density function

Ψ = mode-shape matrix

ω = angular velocity vector

$\tilde{\omega}$ = skew-symmetric matrix of the components of ω

θ = rigidbody rotational coordinate

σ = stress tensor

ϵ = strain tensor

Ω = domain

R = region of ultimate boundedness

R^c = complement of R

Chapter 1

INTRODUCTION

1.1 Literature Survey

Many space missions envisioned for the future will require multibody space systems. Examples of such structures include space platforms with multiple articulated payloads and space-based manipulators for on-orbit assembly and satellite servicing. Such systems are expected to have significant flexibility in the structural members as well as joints. Control systems design for multibody flexible systems is a difficult problem because of the large number of significant elastic modes with low inherent damping and the inaccuracies and uncertainties in the mathematical model. Furthermore, the dynamics of such systems are highly nonlinear. The literature contains a number of important stability results for certain subclasses of this problem; for example, linear flexible structures, nonlinear multibody rigid structures, and most recently multibody flexible structures. Under certain conditions the input-output maps for such systems can be shown to be "passive" [1]. A stability theorem based on Popov's hyperstability concepts [2] states that a passive linear system controlled by a strictly passive compensator is closed-loop stable. The Lyapunov and passivity approaches are used in [3] to demonstrate global asymptotic stability of linear flexible space structures (with no articulated appendages) for a class of dissipative compensators.

These include collocated attitude controllers and collocated damping enhancement controllers. The stability properties were shown to be robust to first-order actuator dynamics and certain actuator/sensor nonlinearities. Multibody rigid structures comprise another class of systems for which stability results have been developed. Ideally, subject to certain restrictions, these systems can be categorized as "natural systems" . Such systems are known to exhibit global asymptotic stability under static dissipative or proportional-and-derivative (PD) control. Upon recognition that rigid manipulators belong to the class of natural systems, a number of researchers, among them [4], [5], [6] and [7] have established global asymptotic stability of rigid manipulators employing PD control with gravity compensation. Stability of tracking controllers was investigated in [8] and [9] for rigid manipulators. In [10] an extension of the results of [8] to the exponentially stable tracking control for flexible multilink manipulators, local to the desired trajectory, was done. Lyapunov stability of multilink flexible systems was addressed in [11].

Many researchers have worked on the stability of dissipative dynamical systems. A detailed study of dissipative dynamical systems was done in [12] and [13]. It seems that there was a parallel development in the state-space approach and the transfer function approach for establishing passivity based theory for linear systems. Most of the noteworthy results were based on the theory of positive-real transfer matrices and their implications on the stability properties of the linear systems having positive-real transfer functions.

The most important result of all, the Kalman-Yacubovich Lemma, establishes the equivalent conditions for positive-realness of a transfer function in terms of the state-space description of the system. Earlier([14]) the positivity-based controllers were formulated for systems with elastic modes only. Later work (see [15]) considers these controllers to control both elastic and rigid body modes of the system. Some researchers studied the stability problem from the input-output perspective

[16], [17]. A significant investigation was also done in [18]- [21] on the stability of nonlinear systems.

1.2 Contributions of this Thesis

The main objective of this dissertation is to extend the stability robustness results existing of linear, flexible space systems to multibody, nonlinear, flexible space systems under dissipative control. As noted in the previous section, much work has been done in the control of linear dissipative systems and the foundation has been laid in the area of dissipative nonlinear systems. In particular, for rigid robotic systems, representing a class of multibody, nonlinear rigid systems, some important stability results were obtained in the 80's. However, the global asymptotic stability for nonlinear, multilink, flexible space-structures under dissipative compensation has not been thoroughly addressed, and that is the subject of this thesis. Essentially, most of the results previously obtained in [3] and [15] for linear systems are extended here to nonlinear systems. First it is shown that flexible multibody systems exhibit asymptotic stability under static dissipative compensation. Furthermore, the effects of realistic nonlinearities in the actuators and sensors are investigated. The proofs given here use Lyapunov's stability theorem along with Lasalle's theorem to prove asymptotic stability. All the proofs exploit inherent passivity of the systems under consideration. The Lyapunov functions used are energy-type functions. In the case of actuator/sensor nonlinearities the proofs use energy-type Lyapunov function augmented with an appropriate positive definite function to prove global asymptotic stability. For systems with linear actuators and sensors, the stability proof by Lyapunov's method can take a simpler form if the Work-Energy Rate principle [11] is used. However, since the work-energy rate principle is applicable only when the system is holonomic and scleronomic in nature, a more direct approach is used in evaluating the time derivative of the Lyapunov function so that the results are more

general and account for the realistic actuator/sensor nonlinearities. Also dynamic dissipative compensators, which are shown to provide the robust stability and offer more design degrees of freedom, constitute the most general class of linear dynamic compensators for the class of systems under consideration.

1.3 Thesis Outline

The organization of the dissertation is as follows.

In Chapter 2, a mathematical model of a class of multibody, nonlinear, flexible space systems is developed. An effort is been made to keep the derivation as general as possible. The model system is assumed to have a branch geometry, so that, it can represent a large class of spacecraft. Kinematic quantities are derived using rotation transformation matrices. The equations of motion are based on the Lagrangian formulation. Finally the chapter is concluded with a theorem which establishes a very important property of the systems under consideration which is focal to the derivations done in the subsequent chapters.

Chapter 3 is aimed at building the necessary theoretical background in the area of dissipative systems. This chapter has essentially three parts. The first part reviews various control design methods that are currently available. The advantages and limitations of these methods are also noted. In particular, it is noted that these methods are not generally applicable to nonlinear systems. In the second part, some definitions related to the dissipativity and passivity are given. This part also reviews some linear system results to date which are instrumental in extending those results to the nonlinear case. The last section in the chapter establishes passivity of the nonlinear systems under consideration for the given supply rate and storage function. Essentially, this chapter lays the foundation for the theoretical development in the next two chapters.

Chapter 4 establishes various stability results for nonlinear, multibody, flexible systems under static dissipative compensation. It is shown that static dissipative controllers result in global, asymptotic stability of these systems. The stability is robust to modeling errors and parametric uncertainties. Furthermore, it also shown that the asymptotic stability property holds even in the presense of certain realistic actuator/sensor nonlinearities. The chapter is concluded with the proof that shows that there exists a finite region of ultimate boundedness in the presense actuator deadzone or hysteresis nonlinearities and system trajectories do not go unbounded.

Chapter 5 extends the asymptotic stability results of chapter 4 to a more versatile class of compensators, namely, dynamic dissipative controllers. The conditions under which a linear dynamic dissipative controller can exhibit global asymptotic stability are derived. The results are very useful since they give the control designer more design degrees of freedom (over static dissipative type) which can be used for performance enhancement.

In Chapter 6 some numerical examples are given to demonstrate some of the theoretical results obtained in Chapters 4 and 5. It is demonstrated that the static dissipative controller stabilizes a nonlinear, multibody, flexible system. A numerical example using dynamic dissipative controller is given for a system which is assumed to be locally linear near its operating points. One application is also given for a linear, flexible, single-body structure.

Finally, some conclusions and possible directions for future research are given in Chapter 7.

Chapter 2

MATHEMATICAL MODEL

The objective of this chapter is to derive, in the most general form, the equations of motion for nonlinear, multibody, flexible, spacecraft. Some examples of these are satellites with flexible appendages such as solar arrays and antennas, the space-shuttle with remote manipulator system (RMS) and flexible space-platforms with multiple articulated payloads (space-station). The approach taken to derive the equations of motion is very general and applies to the systems falling under above mentioned category. The method used to derive the equations of motion is the well known Euler-Lagrange approach. The procedure involves obtaining the Lagrangian of the system, which is the difference of the kinetic and potential energy of the system, and then using Euler-Lagrange equations to derive the dynamical equations of motion.

2.1 Modeling Considerations

The systems under consideration can be schematically represented by the configuration shown in Figure 2.1. The purpose here is to represent a relatively general formulation of the equations of motion. It is assummed that all bodies in the system are flexible. The deformations in the bodies are assumed to be due only to elastic motion; however, any other deformations, such as, due to thermal effects, can also be modeled if required. The system model under consideration has cluster configuration.

It consists of one central body attached to various appendage-bodies to form a branch geometry. For the purpose of derivation following notations are used. Let each body be denoted by B_{ik}, where, the first subscript indicates the branch the body belongs to, and the second subscript indicates the body number in that particular branch. The number and the locations of various bodies are arbitrary so that the system configuration is more general.

2.1.1 Coordinate Systems

Consider Figure 2.2. X_c, Y_c, Z_c is the inertial coordinate system and X_{i0}, Y_{i0}, Z_{i0} is the coordinate system attached to the central body. All other X_{ij}, Y_{ij}, Z_{ij} are local coordinate systems. Each of these local coordinate systems is located at the point of connection between two bodies. The motion of each local coordinate system origin, O_{ij}, is defined with respect to the previous local coordinate frame. In the following section the kinematic quantities, such as, position and velocity, will be derived for any general particle mass at location, say P, will be derived.

2.2 Kinematics

Referring to Figure 2.2, the position vector of a point in a body, in the local reference frame, is given by

$$\overline{s}_{ik} = \overline{a}_{ik} + \overline{\rho}_{ik} \tag{2.1}$$

where, $\overline{a}_{ik}$ is the position vector of the point if the motion was only rigid body motion, and $\overline{\rho}_{ik}$ is the contribution due to the elastic motion. In general, for any particle mass dm at point P in the body n_p of ith branch, the positon vector is given by

$$\overline{r}_{ip} = \overline{r}_{i0} + \sum_{j=0}^{n_p-1} R^c_{ij} \overline{s}_{i(j+1)} \tag{2.2}$$

$$\text{where,} \quad R^c_{ik} = R^c_{i0} R^{i0}_{i1} R^{i1}_{i2} .... R^{i(k-1)}_{ik} \tag{2.3}$$

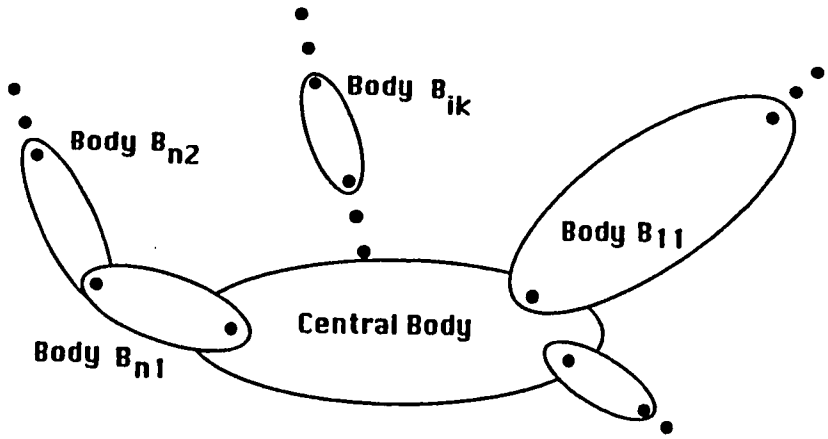

Fig. 2.1 A schematic of the spacecraft model.

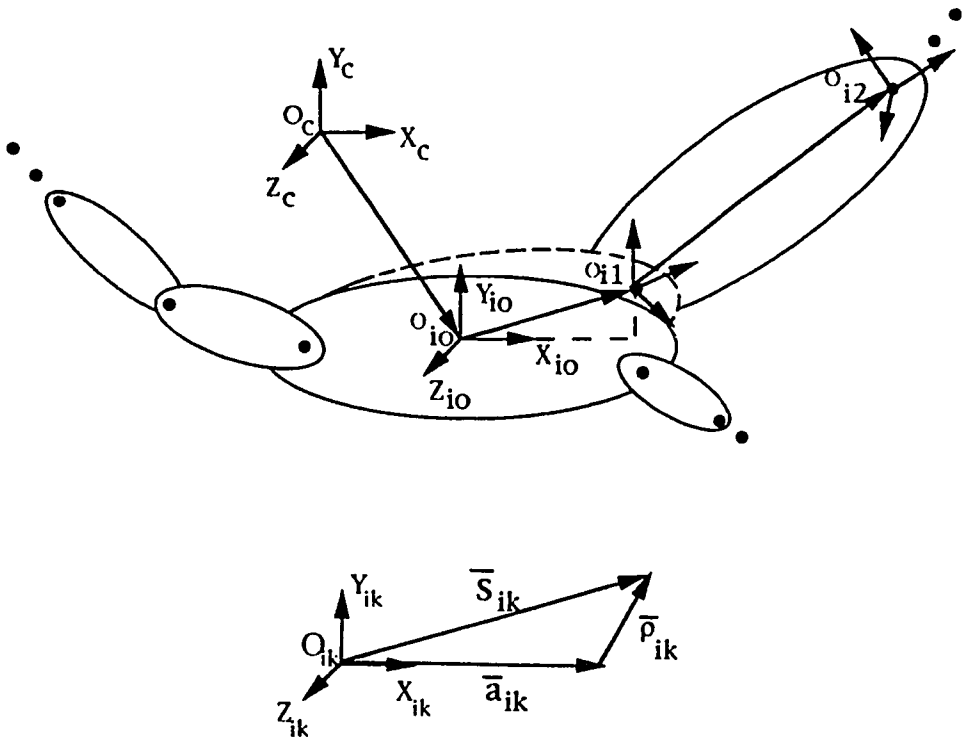

Fig. 2.2 The coordinate systems.

The matrix R^i_j in the above equation is the rotational transformation matrix between frames i and j. Appendix A gives form and properties of these matrices. The velocity of P is then given by taking the time derivative of Eq. 2.3.

$$\dot{\bar{r}}_{ip} = \dot{\bar{r}}_{i0} + \dot{R}^c_{i0}\bar{s}_{i1} + R^c_{i0}\dot{\bar{s}}_{i1} + \dot{R}^c_{i0}R^{i0}_{i1}\bar{s}_{i2} + R^c_{i0}\dot{R}^{i0}_{i1}\bar{s}_{i2} + ... + R^c_{in_p}\dot{\bar{s}}_{in_p} \quad (2.4)$$

$$\dot{\bar{r}}_{ip} = \dot{\bar{r}}_{i0} + \sum_{j=1}^{n_p} \dot{R}^c_{i0}R^{i0}_{ij}\bar{s}_{ij} + \sum_{k=2}^{n_p}\sum_{j=1}^{k} R^c_{i(j-1)}\dot{R}^{i(j-1)}_{ij}R^{ij}_{ik}\bar{s}_{ik} + \sum_{j=0}^{n_p-1} R^c_{ij}\dot{\bar{s}}_{i(j+1)} \quad (2.5)$$

The time derivatives of R and $\bar{s}$ are obtained as follows.

$$\dot{R}^{ij}_{ik}\bar{s}_{ik} = \tilde{\omega}_k R^{ij}_{ik}\bar{s}_{ik} \quad (2.6)$$

$$\dot{R}^{ij}_{ik}\bar{s}_{ik} = -R^{ij}_{ik}\tilde{s}_{ik}\bar{\omega}_k \quad (2.7)$$

$$\dot{\bar{s}}_{ij} = \dot{\bar{\rho}}_{ij} = \sum_{m=1}^{n_m} \phi_{ijm}\dot{q}_{ijm} \quad (2.8)$$

where, n_m is the number of mode shapes to be used and ϕ_{ijm} is the mode shape vector. The notation $\tilde{\omega}$ indicates the "skew symmetric" matrix formed by the elements of vector $\bar{\omega}$. So,if $\bar{\omega} = \{\omega_x, \omega_y, \omega_z\}^T$ then $\tilde{\omega}$ is given by

$$\tilde{\omega} = \begin{bmatrix} 0 & -\omega_z & \omega_y \\ \omega_z & 0 & -\omega_x \\ -\omega_y & \omega_x & 0 \end{bmatrix}$$

Substituting Eqs 2.6, 2.7 and 2.8 in Eq. 2.5 yields

$$\dot{\bar{r}}_{ip} = \dot{\bar{r}}_{i0} - R^c_{i0}(\widetilde{\sum_{j=1}^{n_p} R^{i0}_{ij}s_{ij}})\bar{\omega}_{i0} - \sum_{k=2}^{n_p}\sum_{j=1}^{k} R^c_{i(j-1)}R^{i(j-1)}_{ij}(\widetilde{R^{ij}_{ik}s_{ik}})\bar{\omega}_{ij} + \sum_{j=0}^{n_p-1} R^c_{ij}\Phi_{ij}\dot{\bar{q}}_{ij} \quad (2.9)$$

Now $\dot{\bar{r}}_{ip}$ can be rewritten as

$$\dot{\bar{r}}_{ip} = N\dot{p} \quad (2.10)$$

where,

$$N = \begin{bmatrix} I & -R^c_{i0}(\widetilde{\sum_{j=1}^{n_p} R^{i0}_{ij}s_{ij}}) & -R^c_{i1}(\widetilde{\sum_{j=2}^{n_p} R^{i1}_{ij}s_{ij}}) & -R^c_{i2}(\widetilde{\sum_{j=3}^{n_p} R^{i2}_{ij}s_{ij}}) \\ & & \cdots & R^c_{i(n_p-1)}\Phi_{n_p-1} \end{bmatrix} \quad (2.11)$$

and

$$\dot{p} = [\dot{\bar{r}}_{i0} \;\; \bar{\omega}_{i0} \;\; \bar{\omega}_{i1} \;\; \bar{\omega}_{i2} \;\; \ldots \;\; \bar{q}_{i0} \;\; \ldots \;\; \bar{q}_{in_p}]^T \tag{2.12}$$

The equation 2.10 along with Eqs. 2.11 and 2.12 gives the expression for velocity of any point P in n_pth body of ith branch of the system. Having obtained the expressions for kinematic quantities required, the expressions for kinetic and potential energy of the system can be obtained.

2.3 Dynamics

2.3.1 Kinetic Energy

The kinetic energy of the whole system is given by

$$T = \frac{1}{2}\mu \int_\Omega \dot{\bar{r}}_{ip}^T \dot{\bar{r}}_{ip} dm \tag{2.13}$$

where, μ is the mass density, $\dot{\bar{r}}_{ip}$ is as given in Eq. 2.9 and Ω denotes the domain of integration. Substituting Eq. 2.9 into Eq. 2.13 get

$$T = \frac{1}{2}\mu \int_\Omega (N\dot{p})^T N\dot{p} dm$$

$$T = \frac{1}{2}\mu \int_\Omega \dot{p}^T (N^T N)\dot{p} dm \tag{2.14}$$

This can be rewritten as

$$T = \frac{1}{2}\dot{p}^T M(p)\dot{p} \tag{2.15}$$

where, $M(p)$ is the mass-inertia matrix of the system and is given by

$$M(p) = \mu \int_\Omega (N^T N) dm \tag{2.16}$$

$M(p)$ is symmetric and positive definite matrix.

2.3.2 Potential Energy

The potential energy of the system could be due to many sources; such as, elastic displacement, thermal deformation, etc. The deformations due to thermal effects is not considered in the formulation here, however, it can be easily included in the formulation if desired. Thus, it is assumed that the potential energy has contribution from the strain energy, due to elastic deformations, only. Also, it assumed that the materials under consideration are isotropic in nature and that they obey Hook's law.

Then for the isotropic materials obeying Hook's law, the strain energy differential is given as

$$\delta V = \int_{\Omega} \sigma^T \delta \epsilon d\Omega \tag{2.17}$$

which can be rewritten as

$$\delta V = \int_{\Omega} \Psi d\Omega \tag{2.18}$$

where Ψ is the strain energy density and has the form

$$\Psi = \sigma_{xx}\epsilon_{xx} + \sigma_{yy}\epsilon_{yy} + \ldots + \sigma_{yz}\epsilon_{yz} \tag{2.19}$$

Now, for materials obeying Hook's law, following equality holds.

$$\sigma^T = E\epsilon \tag{2.20}$$

The strain-displacement relation is given by

$$\epsilon = \mathcal{D}u \tag{2.21}$$

where, u is the general displacement vector and $\mathcal{D}$ is the differential operator defined by relations

$$\epsilon_{ij} = \frac{1}{2}\left[u_{i,j} + u_{j,i} + \sum_{k=1}^{3} u_{k,i}^{i,j}\right] \qquad \{i,j = 1,2,3\} \tag{2.22}$$

The vector u can be expressed in terms of modal coordinates as

$$u = \Phi q \tag{2.23}$$

Now, from Eq. 2.21

$$\delta\epsilon = \mathcal{D}\Phi\delta q \tag{2.24}$$

Substituting in δV, get

$$\begin{aligned}
\delta V &= \int_\Omega \sigma^T \delta\epsilon d\Omega \\
&= \int_\Omega \epsilon^T E\mathcal{D}\Phi\delta q d\Omega \\
&= \int_\Omega q^T(\mathcal{D}\Phi)^T E\mathcal{D}\Phi\delta q d\Omega \\
&= q^T\int_\Omega(\mathcal{D}\Phi)^T E\mathcal{D}\Phi d\Omega\delta q \\
&= q^T K\delta q
\end{aligned} \tag{2.25}$$

where, K is called the stiffness matrix of the system and is given by

$$K = \int_\Omega(\mathcal{D}\Phi)^T E\mathcal{D}\Phi d\Omega \tag{2.26}$$

The potential energy of the system is, then given by

$$V = \frac{1}{2}q^T K q \tag{2.27}$$

2.3.3 Equations of Motion

Using Eqs. 2.13 and 2.27 the Lagrangian of the system is formed as

$$L = T - V \tag{2.28}$$

For the purpose of convenience L can be rewritten in the indicial notation as

$$L = K - V = \frac{1}{2}\sum_{i,j} M_{ij}\dot{p}_i\dot{p}_j - V(q) \tag{2.29}$$

The Euler-Lagrange equations for the system can then be derived from

$$\frac{d}{dt}\left(\frac{\partial L}{\partial \dot{p}_k}\right) - \frac{\partial L}{\partial p_k} = F_k \tag{2.30}$$

where, F_k are generalized forces from non-conservative force field. Evaluating the derivatives,

$$\frac{\partial L}{\partial \dot{p}_k} = \sum_j M_{kj}\dot{p}_j \tag{2.31}$$

and

$$\begin{aligned}\frac{d}{dt}\left(\frac{\partial L}{\partial \dot{p}_k}\right) &= \sum_j M_{kj}\ddot{p}_j + \sum_j M_{kj}\dot{p}_j \\ &= \sum_j M_{kj}\ddot{p}_j + \sum_{i,j}\frac{\partial M_{kj}}{\partial p_i}\dot{p}_i\dot{p}_j \end{aligned} \tag{2.32}$$

Also

$$\frac{\partial L}{\partial p_k} = \frac{1}{2}\sum_{i,j}\frac{\partial M_{ij}}{\partial p_k}\dot{p}_i\dot{p}_j - \frac{\partial V}{\partial p_k} \tag{2.33}$$

Thus the Euler-Lagrange equations can be written

$$\sum_j M_{kj}\ddot{p}_j + \sum_{i,j}\{\frac{\partial M_{kj}}{\partial p_i} - \frac{1}{2}\frac{\partial M_{ij}}{\partial p_k}\}\dot{p}_i\dot{p}_j - \frac{\partial V}{\partial p_k} = F_k \qquad k = 1, ..., n \tag{2.34}$$

By interchanging the order of summation and taking the advantage of symmetry, it can be seen that

$$\sum_{i,j}\{\frac{\partial M_{kj}}{\partial p_i}\}\dot{p}_i\dot{p}_j = \frac{1}{2}\sum_{i,j}\{\frac{\partial M_{kj}}{\partial p_i} + \frac{\partial M_{ki}}{\partial p_j}\}\dot{p}_i\dot{p}_j \tag{2.35}$$

Hence

$$\sum_{i,j}\{\frac{\partial M_{kj}}{\partial p_i} - \frac{1}{2}\frac{\partial M_{ij}}{\partial p_k}\}\dot{p}_i\dot{p}_j = \sum_{i,j}\frac{1}{2}\{\frac{\partial M_{kj}}{\partial p_i} + \frac{\partial M_{ki}}{\partial p_j} - \frac{\partial M_{ij}}{\partial p_k}\}\dot{p}_i\dot{p}_j \tag{2.36}$$

The terms

$$C_{ijk} = \frac{1}{2}\{\frac{\partial M_{kj}}{\partial p_i} + \frac{\partial M_{ki}}{\partial p_j} - \frac{\partial M_{ij}}{\partial p_k}\} \tag{2.37}$$

are known as Christoffel symbols. Note that, for each fixed k, we have $C_{ijk} = C_{jki}$.

Also

$$\frac{\partial V}{\partial p_k} = K_{kj}q_j \tag{2.38}$$

Finally, then Euler-Lagrange equations of motion can be written as

$$\sum_j M_{kj}\ddot{p}_j + \sum_{i,j} C_{ijk}\dot{p}_i\dot{p}_j + D_{kj}\dot{p} + K_{kj}p_j = F_k, \qquad (k = 1, 2, ..., n) \tag{2.39}$$

where D is the inherent structural damping matrix and Dp is the vector of nonconservative forces.

In the equations 2.39, there are four types of terms. The first involve the second derivative of the generalized coordinates. The second are quadratic terms in the first derivatives of p, where the coefficients may depend on p. These terms can be further classified into two types. Terms involving a product of the type $\dot{p}^2$ are called *centrifugal*, while those involving a product of the type $\dot{p}_i\dot{p}_j$ where $i \neq j$ are called Coriolis terms. The third type are the ones which involve only the first derivative of the generalized coordinates and they are the dissipative forces due to the inherent damping. The fourth type of terms involve only p but not its derivatives. These arise from differentiating the potential energy. In the matrix-vector notation, the Eqs. 2.39 are written, in compact form, as

$$M(p)\ddot{p} + C(p,\dot{p})\dot{p} + Dp + Kp = F \tag{2.40}$$

The k,j-th element of the matrix $C(p,\dot{p})$ is defined as

$$\begin{aligned} c_{kj} &= \sum_{i=1}^{n} c_{ijk}(p)\dot{p}_i \\ &= \sum_{i=1}^{n} \frac{1}{2}\{\frac{\partial M_{kj}}{\partial p_i} + \frac{\partial M_{ki}}{\partial p_j} - \frac{\partial M_{ij}}{\partial p_k}\}\dot{p}_i \end{aligned} \tag{2.41}$$

Now, an important property of the systems whose equations of motion are given by 2.40, is derived which is very pivotal to various stability results given in the following chapters.

Theorem 2.1 *The matrix $\dot{M}(p) - 2C(p,\dot{p})$ is skew symmetric.(i.e. if we define the matrix $\mathcal{S}(p,\dot{p}) = \dot{M}(p) - 2C(p,\dot{p})$, then, the components n_{jk} of $\mathcal{S}$ satisfy $n_{jk} = -n_{kj}$.*

Proof 2.1 *The kj-th component of the time derivative of the inertia matrix, $\dot{M}(p)$ is given by the chain rule as*

$$\dot{M}_{kj} = \sum_{i=1}^{n} \frac{\partial M_{kj}}{\partial p_i}\dot{p}_i$$

Therefore, the kj-th component of $S = \dot{M} - 2C$ *is given by*

$$\begin{aligned} \mathcal{S}_{kj} &= \dot{M}_{kj} - 2C_{kj} \\ &= \sum_{i=1}^{n} \left[\frac{\partial M_{kj}}{\partial p_i} - \{ \frac{\partial M_{kj}}{\partial p_i} + \frac{\partial M_{ki}}{\partial p_j} - \frac{\partial M_{ij}}{\partial p_k} \} \right] \dot{p}_i \\ &= \sum_{i=1}^{n} \left[\frac{\partial M_{ij}}{\partial p_k} - \frac{\partial M_{ki}}{\partial p_j} \right] \dot{p}_i \end{aligned} \tag{2.42}$$

Since the inertia matrix is symmetric, i.e., $M_{ij} = M_{ji}$*, it follows from 2.42 by interchanging the indices k and j that*

$$\mathcal{S}_{jk} = -\mathcal{S}_{kj}$$

This completes the proof.

Equation 2.40 will be the governing dynamical equation of motion for the class of systems considered in this report and will be used later in Chapters 3 and 4 as representative mathematical model.

Chapter 3

DISSIPATIVE CONTROLLERS

3.1 Introduction

Over the past two decades, considerable research has been performed on the control of linear, flexible, space systems. Examples of such systems include communication satellites, Earth observation systems, solar power satellites, etc., which are operating in a linear range about a steady-state. The main control problem with these systems is that of controlling the zero-frequency, rigid body modes and suppressing the elastic vibrations [3]. Typically, these systems have a large number of low frequency, closely-spaced modes, inherently low structural damping (i.e. very small energy dissipation), and high degree of uncertainty in their models. In addition, exact mathematical models are not available and the approximate models developed have significant errors. All these factors make it necessary to design a controller which is not only robust to the unmodeled dynamics, but also to the parametric uncertainties. One common controller design approach is the "model-based" controllers. Typically, these controllers use a design model which is of reduced order. This approach is routinely used for controlling relatively rigid spacecraft, wherein only rigid modes are retained in the design model. Second-order notch filters are often incorporated to attenuate the contribution of elastic modes. This approach is generally not advisable

when large number of elastic modes are prominent. Fig. 3.1 shows the effect of using a truncated design model. In building a control loop around the "controlled" modes (the modes used in the design model), a feedback loop is also inadvertantly built around the truncated ("residual") modes. The resulting control system may cause the closed-loop system to be unstable. The unintentional excitation of residual modes and unwanted contribution of the residual modes in the sensed output is termed, in the control literature, as "controll spillover" and "observation spillover". The spillover problem may cause significant reduction in the performance, and even instability leading to the major failures. In view of this, the straightforward use of model-based controllers is inherently limited, and additional techniques must be used to obtain robustness.

At this point it may be worthwhile to look at the various control design methods, starting from classical control techniques up to the most recent, H_∞ design techniques, available to a control designer and the advantages and shortcomings of these methods.

3.2 Survey of Control Design Methods

The history of the control system design goes back to the classical control theory which was based on methods developed by Nyquist and Bode. Classical control theory was best suited for SISO (single-input single-output) linear time-invariant systems. In classical control theory the design is based on the transient response and frequency response characteristics of the system. However, classical control theory had severe limitations and difficulties for design of multivariable control systems and time varying control systems. The so-called modern control theory, which uses the state-space approach, gained popularity in the sixties after the advent of computers. The modern control theory can be applied to the design of linear, multivariable control systems and linear, time-varying control systems that are optimal for given performance indices.

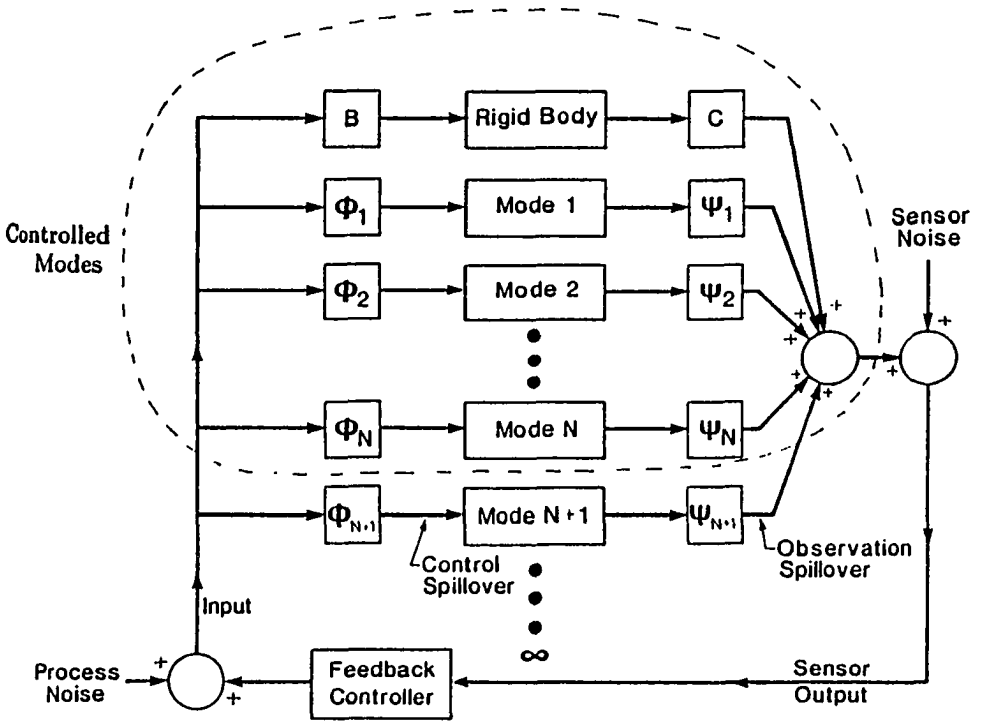

Fig. 3.1 Effect of modal truncation

However, there were many advantages of classical control techniques which were not possessed by modern control theory. For example, the characterization of a complex system is more easily done in terms of frequency response curves since frequency response tests are simple and can be made fairly accurately. The classical methods were extended to the multivariable case in the eighties, using frequency-domain singular value techniques. This area, which includes H_∞ and μ-synthesis methods, is currently an active area of research.

3.2.1 LQG Methods:

With the study of state-space approach to multi-input multi-output systems, the problem of optimal control design attracted the attention of control designers which led to the linear-quadratic-Gaussian (LQG) theory. LQG controllers are basically optimal controllers designed for minimizing a quadratic integral criterion (performance index) based on the performance specifications. Full details on the LQG design techniques can be obtained in various texts (for example see [22], [23], [24], etc.) Recent advances in these methods [28] allow the designer to shape the principal gains (i.e., the singular value frequency response) of the return ratio, at either the input or the output of the plant, to achieve required performance or robustness specifications. The problem addressed by the LQG method is the following.

Suppose a plant model in the state-space form is given by

$$\dot{x} = Ax + Bu + \Gamma w \tag{3.1}$$

$$y = Cx + v \tag{3.2}$$

where w and v are white noise, i.e., zero-mean Gaussian stochastic processes, which are uncorrelated, having covariances

$$E\{ww^T\} = W \geq 0, \qquad E\{vv^T\} = V > 0 \tag{3.3}$$

and

$$E\{wv^T\} = 0 \tag{3.4}$$

In Eq. 3.1 u represents the vector of control input and in 3.2 y represents the measured outputs. The LQG problem is then to find the control law which minimizes the cost

$$J = \lim_{T\to\infty} E\{\int_0^T (z^T Q z + u^T R u)dt\} \tag{3.5}$$

where

$$z = Mx \tag{3.6}$$

is some linear combination of the states, and

$$Q = Q^T \geq 0, \qquad R = R^T > 0 \tag{3.7}$$

are weighting matrices.

The solution to the LQG problem, which uses the *separation principle* [22] (p.390), is then achieved by the following procedure. An optimal estimate $\hat{x}$ of the state x is first obtained, and then this estimate is used (assuming it is the exact measurement of x) to solve the linear quadratic regulator problem. This procedure essentially reduces the problem in two sub-problems, the solutions to which are known. The solution to the first problem, i.e. estimation of the state, is given by Kalman-filter theory. Figure 3.2 shows the block diagram of Kalman filter. It has the structure of state estimator except that the gain matrix K_f is obtained differently. Note that the inputs to the Kalman filter are the plant input and output vectors, u and y, and that its output is the state estimate $\hat{x}$.

The second sub-problem is to find the control signal which minimizes the (deterministic) cost

$$\int_0^\infty (z^T Q z + u^T R u)dt$$

with the assumption that

$$\dot{x} = Ax + Bu$$

The solution is the control signal u given by

$$u = -K_c x$$

where K_c is the feedback gain matrix. The optimal state-feedback matrix K_c is given by

$$K_c = R^{-1}BTP_c \tag{3.8}$$

where P_c satisfies the algebraic Riccati equation (ARE)

$$A^T P_c + P_c A - P_c B R^{-1} B^T P_c + M^T Q M = 0 \tag{3.9}$$

and $P_c = P_c^T \geq 0$. The Kalman-filter gain matrix K_f is given by

$$K_f = P_f C^T V^{-1} \tag{3.10}$$

where P_f satisfies another ARE which is dual to 3.9

$$P_f A^T + A P_f - P_f C^T V^{-1} C P_f + \Gamma W \Gamma^T = 0 \tag{3.11}$$

and $P_f = P_f^T \geq 0$. The matrices K_c and K_f exist, provided that the systems with state-space realizations $(A, B, Q^{1/2}M)$ and $(A, \Gamma W^{1/2}, C)$ are stabilizable and detectable. Also, the matrices P_c and P_f are the unique, symmetric positive definite solutions to the equations 3.9 and 3.11 respectively. Several algorithms are available to solve Eqs. 3.9 and 3.11.

The problem formulation given above, however, does not capture various aspects of the control problem such as, model uncertainties, non-linearities, various kinds of disturbances and possibly many constraints on the realistic solutions, none of which can easily be given mathematical representation. The most that can be done, is the simultaneous tuning of a large number of weighting parameters in matrices Q, R, V and W. In addition, the stability robustness properties with respect to inaccuracies in the modal parameters could not be properly assessed because it is difficult to effectively characterize the bounds on modeling errors in a time-domain setting. It

was shown in [25] that LQG designs can exhibit arbitrarily poor stability margins. One possible remedy is to make the observer dynamics much faster than the desired state-feedback dynamics. However, it was again shown in [26] that this remedy does not work. The LQG/LTR method offers an approach to overcome some of these problems in the frequency domain.

3.2.2 LQG/LTR Method:

This method offers a way of designing the Kalman filter so that the full-state feedback properties are recovered at the input of the plant. It essentially involves placing some of the filter's eigenvalues at the zeros of the plant and the remaining eigenvalues are allowed to become arbitrarily fast. The procedure adopted to design controller by this method [27], [28] is as follows:

Step 1. Define a "design" model of the nominal plant which is an acceptable low frequency representation. Define the high frequency uncertainty (robustness) barrier and the low frequency performance barrier.

Step 2. Design a full state feedback controller based on the steady-state Kalman-Bucy filter. This assumes that the loop is broken at the plant output. Adjust the weighting matrices in the KBF design until its frequency response meets the robustness specifications at low frequencies.

Step 3. Design an LQ regulator to asymptotically "recover" the frequency response obtained in Step 2.

Step 4. Verify stability, robustness, and performance for the entire closed-loop system.

Thus, the LQG/LTR approach requires the characterization of the uncertainty in terms of a frequency-dependent upper bound. However, the performance of this technique is inherently limited since the LQG/LTR method does not account for the uncertainties in the parameters of the design model. Also the loop recovery techniques (LQG/LTR) are not suited for incorporating additive uncertainties. Since

the procedure relies on cancellation of some of the plant dynamics (particularly zeros) by the filter dynamics, it is guaranteed to work only for minimum-phase plants. If right-half plane zeros exist in the plant, then this method may or may not work depending on whether these zeros lie beyond the operating bandwidth of the system, finally designed. Hence, the successful loop recovery may not necessarily give sufficient stability robustness to plant uncertainties. This problem is successfully handled by structured singular value (μ-synthesis) design techniques.

Even if the full state feedback loop gains were recovered exactly, it would only ensure good robustness at input or output only, and not to the actual uncertainties, which are not limited to input and output.

3.2.3 H_∞ and μ-Synthesis Method:

This relatively new approach to the feedback design has been considered as a major breakthrough in the feedback control methodology. The fundamental aspects of the technique are described below. The main idea is based on the fact that any uncertain plant under feedback control can be represented by Fig. 3.3, where P is the modified nominal plant and K is the controller. P and K are known accurately and any uncertainties have been pulled out into a block-diagonal system Δ. The transfer function from the external disturbance w to controlled output z, denoted as T_{zw}, is given by lower linear fractional transformation [30], denoted by $F_l(P,K)$, so that

$$z = T_{zw}w = F_l(P,K)w \tag{3.12}$$

Then, the standard optimization problem for robust performance is defined as [29]:

$$\begin{array}{l}\text{minimize} \\ \text{K, D}\end{array} \quad \|DF_l(P,K)D^{-1}\|_\infty \tag{3.13}$$

where D is a block-diagonal matrix with the same structure as Δ. The significance of this formulation is one can achieve robust stability and performance despite uncertainties. The minimization is done over all realizable controllers $K(s)$ which stabilize

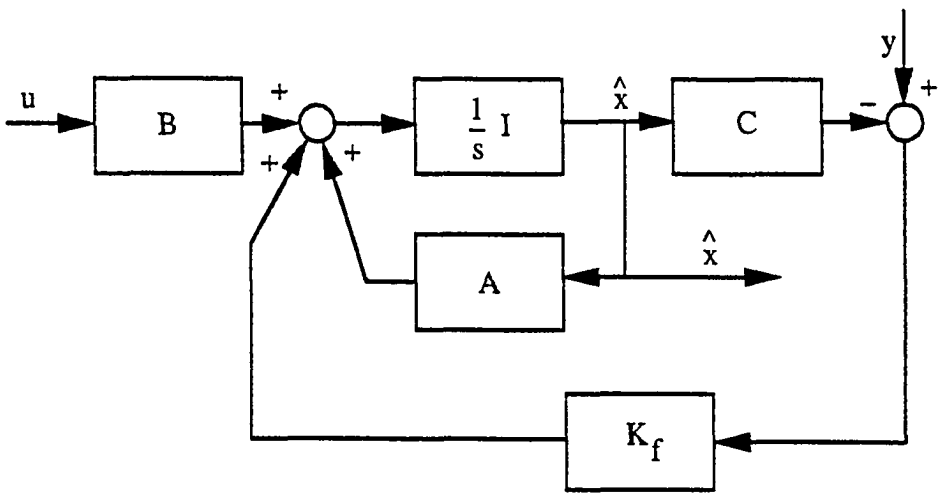

Fig. 3.2 Kalman-filter: block diagram

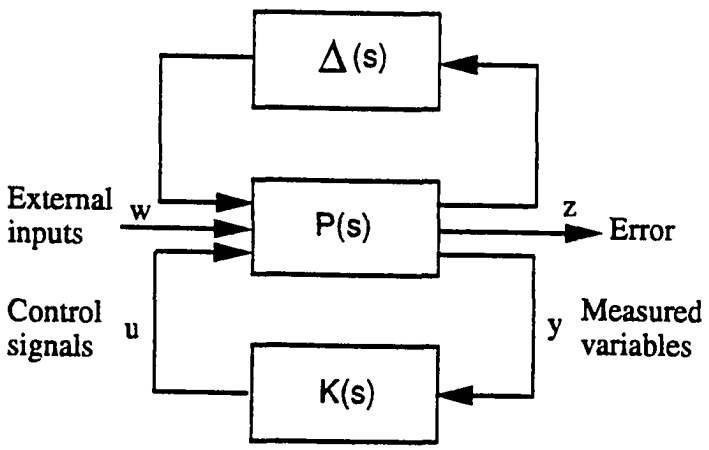

Fig. 3.3 A standard representation of an uncertain plant

the closed loop and over all Ds. To date only approximate methods are available for solving Eq. 3.13. The minimization problem given by Eq. 3.13 is solved by iteratively solving for D and K. With fixed D it becomes a standard H_∞ problem and with fixed K the minimization over D is convex, so at worst it can be performed by search techniques.

The Glover-Doyle algorithm [31] is used to solve the H_∞ problem for fixed D. This approximate solution is known to give good results. However, this iterative scheme is known to have failed for certain problems. Also, numerical problems are quite formidable and the solutions obtained are quite conservative since the uncertainties are modeled as complex-valued, i.e, Δ is assumed to be complex. The parallel between the LQG method and H_∞ method is, both methods require solving two AREs, however, LQG method requires characterization of noise and LQG solutions are over smaller domain.

3.2.4 Dissipative Controllers: A Remedy?

In summary, the H_∞/μ-synthesis design technique overcomes many of the difficulties of structural control including spillover problem and nonminimum phase transmission zeros (note that, this was a limitation of LTR). However, in the case of flexible, light-weight space structures, which have numerous low-frequency, poorly damped modes, H_∞ and μ-synthesis design may be very conservative. Furthermore, for nonlinear systems, LQG, LQG/LTR and H_∞/μ-synthesis techniques are not applicable. In [33] it was shown that for linear flexible structures an attractive alternative is offered by "*dissipative controllers*". The only property required for guaranteed stability robustness with dissipative controllers is that the I/O map of the plant is passive. In the case of linear systems, these controllers are known to be robust to uncertainties and modeling errors. In the recent past, much work has been done in developing the theory of dissipative controllers for linear dynamical systems. Dissipative controllers

also offer the possibility of extension to nonlinear passive systems. It seems appropriate to review some background material on the disspative systems to help understand the theoretical developments given in the subsequent chapters.

The organization of the remainder of this chapter is as follows. In the first few sections some important definitions, as regards to the dissipativity and passivity, are given in the context of linear as well as nonlinear systems. Then, in the following sections, some key stability results, existing for linear systems under dissipative compensation, are noted. Finally, the passivity property of nonlinear systems for given supply rate function is established.

3.3 Dissipativity and Passivity

Some basic concepts related to the notions of dissipativity and passivity are reviewed below. These concepts are necessary to understand the theories developed in the subsequent chapters.

3.3.1 Mathematical Preliminaries

Following are some mathematical terminologies and notations, that will be needed.

Let us suppose that the dynamical system, denoted by Σ, is defined through the sets $U, \mathcal{U}, Y, \mathcal{Y}, X$ and the maps ϕ and r, which are defined as follows:

(i) $\mathcal{U}$ is called the *input space* and consists of a class of U-valued functions on R. The set U is called the set of input values.

(ii) $\mathcal{Y}$ is called the *output space* and consists of a class of Y-valued functions on R. The set Y is called the set of output values.

(iii) X is an abstract set called the *state space.*

(iv) ϕ is called the *state transition function* and is a map from $R \times X \times U$ into X, i.e. $x = \phi(x_0, t, u)$.

(v) r is called the *read-out function* and is a map from $X \times U$ into Y.

Supply Rate, Dissipation Inequality and Available Storage

Definition 1.: Let w be the real valued function, called the *supply rate*, defined on $U \times Y$. It is assumed that for any $\mathcal{U} \in U$ and any $\mathcal{Y} \in Y$ the function $w(t) = w(y(t), u(t))$ satisfies

$$\int_0^\infty w(t)dt < \infty \qquad \text{for all} \quad t \geq 0$$

Definition 2.: A dynamical system with supply rate w is said to be dissipative if there exists a nonnegative function $V : X \rightarrow R$, called the *storage function*, such that for all $\mathcal{U} \in U$, $x_0 \in X$, and $t \geq 0$

$$V(x) - V(x_0) \leq \int_0^t w(t)dt$$

where $x = \phi(t, x_0, u)$. The above inequality is called the *dissipation inequality.*

Definition 3.: The *available storage*, $V_a : X \rightarrow R$, of a system Σ with supply rate w is defined as

$$V_a(x) \;=\; \sup_{\substack{t \geq 0 \\ x_0 = x \\ u \in \mathcal{U}}} \; \{ - \textstyle\int_0^t w(t)dt \}$$

Definition 4.: If a system Σ with supply rate w is dissipative, the *available storage* V_a is finite for all $x \in X$. Moreover, the storage function V satisfies

$$0 \leq V_a(x) \leq V(x)$$

for each $x \in X$ and V_a itself is a possible storage function.

Truncations, Extended Spaces

Definition 5.: For $p \in [1, \infty)$, the set $L_p = L_p[0, \infty)$ denotes the set of all functions $f(.)$ in X such that the function $t \rightarrow [|f(t)|]^p$ is integrable over $[0, \infty)$. i.e.

$$f(.) \in L_p \quad \text{for a fixed} \quad p \in [1, \infty) \quad \text{iff} \quad \int_0^\infty [|f(t)|]^p dt < \infty$$

Definition 6.: Let $T < \infty$; then the truncation operator $P_T : X \rightarrow X$ is defined by setting

$$(P_T X)(t) = \begin{cases} x(t) & t \in [0,T] \\ 0 & t > T \end{cases} \qquad \forall x \in X$$

For brevity the function $P_T x$ is denoted as x_T.

Definition 7.: For a fixed $p \in [1, \infty]$, the symbol $L_{pe} = L_{pe}[0, \infty)$ denotes the set of all functions $f(.)$ in X such that $f_T(.) \in L_p \quad \forall \quad T < \infty$. (Note that $f(.)$ itself may or may not belong to L_p). The space L_{pe} is called as the extension space of L_p.

Definition 8.: Let $p \in [1, \infty]$ be fixed, and let $T < \infty$. Then for every $f \in L_{pe}$, the truncated norm $\|f\|_{Tp}$ is defined by

$$\|f\|_{Tp} = \|f_T\|_p = \|P_T f\|_p$$

Let $p = 2$, and let $T < \infty$. Then for every $f, g \in L_{2e}$, the truncated inner product $< f, g >_T$ is defined by

$$< f, g >_T = < f_T, g_T > = \int_0^T f(t)g(t)dt$$

The important thing to note here is that, for every $p \in [1, \infty]$ and every $f \in L_{pe}$, the quantity $\|f\|_{Tp}$ is a well-defined finite real number for every $T < \infty$, though $\|f\|_p$ is defined only if f actually belongs to the unextended space L_p.

For the multi-input multi-output case the above definitions are modified to introduce the spaces L_p^n and L_{pe}^n.

Definition 9.: Let $p \in [1, \infty]$ and let $n \geq 1$ be an integer. Then the set L_p^n (respectively L_{pe}^n) consists of all n-tuples $\overline{f}(.) = [f_1(.) \quad f_2(.) \quad ... f_n(.)]'$, where $f_i(.) \in L_p$ (respectively in L_{pe} $\forall i$. The norm of a function $\overline{f}(.) \in L_p$ is defined by

$$\|\overline{f}(.)\|_p = \begin{cases} \{\int_0^\infty \|f(t)\|^p dt\}^{\frac{1}{p}} & \text{if} \quad p < \infty, \\ \underset{t \in [0,\infty)}{\text{ess.sup}} \|f(t)\| & \text{if} \quad p = \infty \end{cases}$$

where $\|\cdot\|$ is the Euclidean norm on R^n.

The truncated norm $\|.\|_T : L_{pe}^n \rightarrow R$ and the truncated inner product $< ., . >_T$: $L_{2e}^n \rightarrow R$ are defined in a manner analogous to the definition 8.

3.3.2 Dissipative Linear Dynamical Systems

Introduction

Since it is a great deal easier to deal with the nonlinear systems after better understanding of linear system results, this section is devoted to the study of dissipative linear system results existing to date. The dissipativity of the system in the context of linear dynamical systems and their consequences on the stability properties of the system are studied. After reviewing the existing results on the conditions for dissipativeness for such systems the results on the dissipative controller design for linear systems are given. The supply rate functions that are of interest here are quadratic functions, and the one with primary focus would be

$$w =< u, y >= u'y$$

It is to be noted that the other type of supply rate functions in u and x are also possible. The consequences of the linear dynamical system being dissipative with respect to the supply rate w, given above, have been studied by many researchers and some established results are presented below. A thorough treatment of the dissipative linear systems can be found in [12], [13], [17], and many other places. An effort is made to be concise, yet elaborate enough, in covering the background material to help understand the concepts and motivation behind the work presented in the subsequent chapters.

Dissipativity and Passivity

This section defines the concepts of dissipativity and passivity, which can only be applied to operators $H : L_{2e}^n \rightarrow L_{2e}^m$. For the simplicity, it is assumed that $m = n$. Note that, this will be tha case for collocated actuators and sensors. "Dissipativity" of an operator is an input-output property and is formally defined in the system theory literature (for example, see [17], [15]) as follows:

Definition 10.- Let $\mathbf{H}$:$L_{2e}^n \rightarrow L_{2e}^n$, where L_{2e}^n denotes the extended Lebesgue space as defined in [6]. and suppose Q, R,S are $n \times n$ matrices with Q and S symmetric. Then the operator $\mathbf{H}$ is said to be "(Q, R, S)-dissipative" if

$$< \mathbf{H}x, Q\mathbf{H}x >_T + < x, Rx >_T +$$

$$< \mathbf{H}x, Sx >_T \geq 0, \quad \forall T \geq 0, \quad \forall x \varepsilon \mathbf{L}_{2e}^n \tag{3.14}$$

($< ., . >_T$ denotes the L_{2e}^n -inner product).

Various stability results for systems satisfying this general dissipativity definition can be found in the literature. However, the practical usefulness of many of these results is rather limited because the stability depends on the system parameters, and not solely on the dissipativity. A special case of dissipativity, wherein Q and R are zero and S = I, is called "passivity". That is, $\mathbf{H}$ is said to be passive if it is "$(0_n, 0_n, I_n)$- dissipative. H is said to be "strictly passive" if it is dissipative with respect to $(0_n, -\epsilon I_n, I_n)$ for some $\epsilon > 0$, i.e., if

$$< x, \mathbf{H}x >_T \geq \epsilon \|x\|_T^2, \quad \forall T \geq 0, \quad \forall x \in L_{2e}^n$$

In the frequency-domain, the definitions of passivity and strict passivity take an equivalent form which relates to the "positive realness" and "strictly positive realness",respectively, of the transfer function of the system.

Definition 11.-A square transfer function $Z(s)$ is called positive-real if (i) $Z(s)$ is real for real s (ii) $Z(s)$ is analytic for $Re[s] > 0$ (iii) $Z^*(s) + Z(s)$ is non-negative definite for $Re[s] > 0$ (* denotes the complex conjugate transpose)

Definition 12. A square transfer function $Z(s)$ is "strictly positive-real" if (i) $Z(s)$ is real for real s (ii) $Z(s)$ is analytic for $Re[s] > 0$ (iii) $Z^*(j\omega) + Z(j\omega)$ is non-negative definite for all real ω

A considerable amount of literature is available on the use of positive-real matrices in the system theory. Many researchers have expanded on the basic stability theorem based on Popov's hyperstability concept [2]. Referring to the Fig. 3.4,

the conditions for the stability based on the positivity arguments are given by the following theorem [2] [14],

Theorem 3.1 *If in the feedback configuration shown in the Fig. 3.4, $G(s)$ and $K(s)$ are square transfer matrices, then the closed-loop system is asymptotically stable if at least one of the transfer matrices is positive-real and the other is strictly positive-real.*

Proof 3.1 *The proof can be found in [14].*

Some of the worthy literature based on the theory of positive-real transfer matrices, and their implications on the stability of the linear systems having positive-real transfer functions can be found in [2], [34], [38], [14], [35], etc. Before closing this section one important result [34], in the literature known as Kalman-Yacubovich lemma, is given. This gives the equivalent condition for the positive-realness of the transfer function in terms of the state-space matrices.

Suppose $(\mathcal{A}, \mathcal{B}, \mathcal{C}, \mathcal{D})$ is an nth order minimal realization of $G(s)$. Then, a necessary and sufficient condition [34] for $G(s)$ to be positive-real is that there exists an $n \times n$ symmetric positive definite matrix P, and matrices W and L such that

$$\begin{aligned} \mathcal{A}^T P + P\mathcal{A} &= -LL^T \\ \mathcal{C} &= \mathcal{B}^T P + W^T L \\ W^T W &= \mathcal{D} + \mathcal{D}^T \end{aligned} \tag{3.15}$$

3.4 Dissipative Controllers

In view of the background covered in the earlier sections, the term "dissipative controllers", is defined here. As the name suggests, these controllers are based on the concept of dissipation of energy. Numerous references can be given (for example, see [2], [3], [12], [13], [17], etc.) for the work done in the area of stability properties of linear dissipative systems.

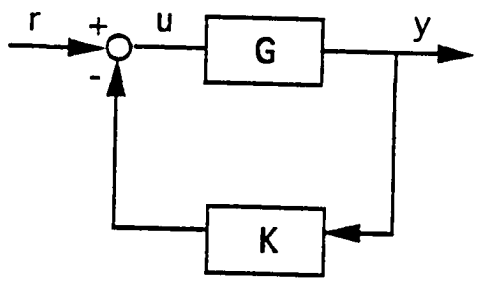

Fig. 3.4 Feedback configuration

Dissipative controllers basically use collocated compatible actuators and sensors. They employ output feedback and therefore they are easy to implement. It will be shown that, the closed-loop stability is guaranteed in the presense of parametric uncertainties as well as some realistic actuator/sensor nonlinearities. Since the controllers are not model-based and plant models are used only for optimizing control performance, they provide excellent stability robustness. The stability results are based on the concept of "energy dissipation" in the closed-loop feedback system.

Essentially, dissipative controllers are related to positivity-based controllers [14], but are significantly different from the latter because they are designed to control both rigid (zero-frequency) modes and elastic modes, and because they use feedback of both position (attitude) and rate. For the special case where rigid modes are not present (e.g., a ground test article) and only velocity sensors are used, the dissipative controller degenerates to a positivity controller.

3.4.1 Types of Dissipative Controllers

There are following different types of dissipative controllers.

(i) constant gain or *static dissipative* controllers

(ii) linear, time-invariant, *dynamic dissipative* controllers

(iii) linear, time varying and nonlinear dissipative controllers

A thorough treatment of the first two types for linear time invariant (LTI) space systems can be found in [3] and [15]. Following two sections will review some of the key results established for linear systems.

3.4.2 Static Dissipative Controllers for LTI systems

Consider a LTI system

$$A_s\ddot{p} + B_s\dot{p} + C_s p = \Gamma^T u$$

where

$$p = (\alpha^T, q^T)^T, \qquad A_s = diag[J_s, I_{nq}], \qquad B_s = diag[0_3, D_{n_q \times n_q}] \tag{3.16}$$

$$C_s = diag[0_3, \Lambda_{n_q \times n_q}], \qquad \Lambda^T = \begin{bmatrix} I_3 & \cdots & I_3 \\ \Phi_1^T & \cdots & \Phi_{m_T}^T \end{bmatrix} \tag{3.17}$$

$$y_p = \Gamma p \qquad y_r = \Gamma \dot{p} \tag{3.18}$$

This system represents the rigid-body rotational dynamics and the elastic motion of a linearized model of a flexible spacecraft with no articulated appendages [3]. For example, this model can represent a large flexible space antenna, wherein y_p and y_r denote attitude and rate measurement vectors and u denote the control torque vector(applied at the same locations). The constant-gain or static dissipative control law is given by:

$$u = -G_p y_p - G_r y_r$$

where G_p and G_r are symmetric, positive-definite, proportional and rate gain matrices. It has been shown [3] that this control law gives guaranteed asymptotic stability (of the entire system consisting of both rigid and flexible modes) regardless of unmodeled elastic modes or parameter uncertainties. (It was also shown in [3] that stability is maintained even if small imprecision exists in the collocation of the actuators and sensors).

Robustness to Actuator/Sensor Nonlinearities

In practice, the devices available for actuation and sensing are not perfect (i.e., they are not linear and instantaneous). They have nonlinearities and phase lags. Some of the commonly occured nonlinearities are: saturation delays, relays, dead-zones, hysteresis, and many other sector nonlinearities. The control designer has to ensure that the controller is robust to these nonlinearities. The saturation nonlinearity is very commonly observed in the actuators and is as shown in Fig. 3.5. It can be seen that the output of the actuator, $\psi(\nu)$, is linear in the region $(-\nu_s, +\nu_s)$ and constant

outside the region. Fig. 3.6 shows another type of nonlinearity, called dead-zone nonlinearity. In this type of nonlinearity there is a deadband, in figure $(-\delta, +\delta)$, inside of which there is no output from the actuator. This type of nonlinearity presents a major problem in achieving asymptotic stability of the origin. Figures 3.7 and 3.8 show, respectively, $[0, \infty)$-sector monotonically increasing nonlinearity and $(0, \infty)$-sector nonlinearity[Note: A single-valued function $\psi(\nu)$ is said to belong to the $(0, \infty)$ sector if $\psi(0) = 0$ and $\nu\psi(\nu) > 0$ for $\nu \neq 0; \psi$ is said to belong to the $[0, \infty)$ sector if $\nu\psi(\nu) \geq 0$].

In [3] it was also shown that, if G_p and G_r are diagonal, the robust stability property of static dissipative controllers is carried over in the presence of:

1) monotonically increasing actuator nonlinearities, rate sensor nonlinearities belonging to the $[0, \infty)$-sector, and position sensor nonlinearities belonging to the $(0, \infty)$-sector, and

2) stable actuator dynamics $g_a(s) = k/(s+a)$, provided that $g_p/g_r < a$, where g_p and g_r denote the appropriate diagonal elements of G_p and G_r.

The gains, G_p and G_r, can be designed to minimize a quadratic performance function or to obtain closed-loop eigenvalues close to the desired locations in the least-square sense [3]. However, a drawback of these controllers is that the performance may be inherently limited because of the structure of the controller.

3.4.3 Dynamic Dissipative Controllers for LTI systems

In order to obtain better performance while still retaining the guaranteed robustness to unmodeled dynamics and parameter uncertainties, a class of dynamic dissipative controllers (DDC) is suggested. Such controllers had been suggested in the past for controlling only the elastic motion [14], [36], [37]. These controllers are based on the fact that the "plant", consisting only of the elastic modes and with velocity measurements as the output, is "passive" [or equivalently, the transfer function is

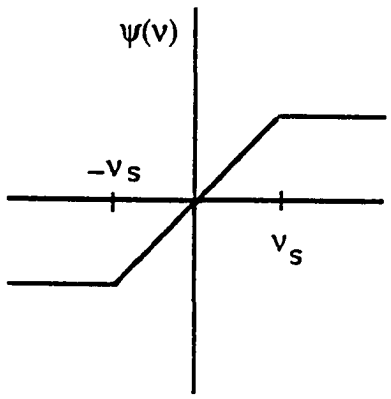

Fig. 3.5 Saturation nonlinearity

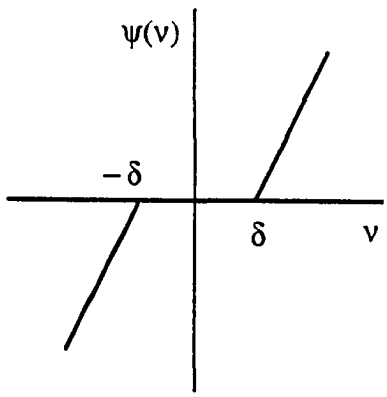

Fig. 3.6 Dead-zone nonlinearity

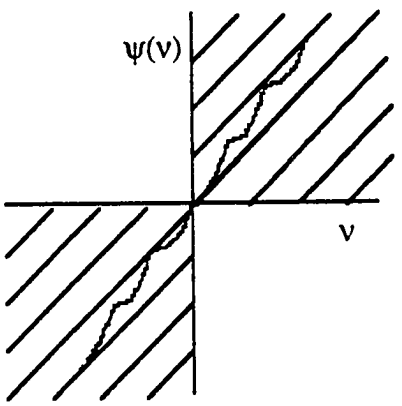

Fig. 3.7 $[0, \infty)$-sector monotonically increasing nonlinearity

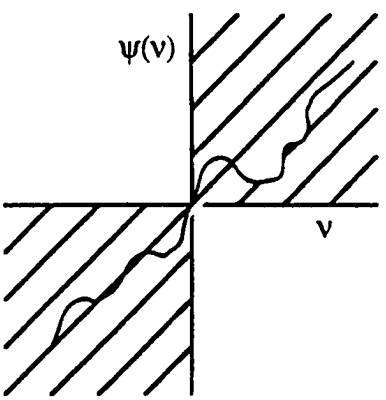

Fig. 3.8 $(0, \infty)$-sector nonlinearity

"positive-real"]. Then theorem 3.1 was used to design the controller. However, in [39], a DDC was presented for controlling both rigid and elastic modes. An extenssion to the multivariable case was done in [15]. One important result from [15] is given below which establishes the asymptotic stability of dynamic dissipative controllers for LTI systems under consideration.

Consider a feedback configuration shown in Fig. 3.9. Let a controller $K(s)$ be represented by the minimal realization

$$\begin{aligned} \dot{x}_k &= A_k x_k + B_k u_k \\ y_k &= C_k x_k + D_k u_k \end{aligned} \tag{3.19}$$

Now, define

$$\begin{aligned} \dot{v} &= y_k \\ z &= (x_k^T, v^T)^T \\ y_c &= v \end{aligned} \tag{3.20}$$

Equations 3.19 and 3.20 can be combined as:

$$\dot{z} = A_z z + B_z u_k$$

$$y_c = C_z z$$

where

$$A_z = \begin{bmatrix} A_k & 0 \\ C_k & 0 \end{bmatrix} \quad B_z = \begin{bmatrix} B_k \\ D_k \end{bmatrix} \quad C = \begin{bmatrix} 0 & I_3 \end{bmatrix} \tag{3.21}$$

Theorem 3.2 *Consider plant $G(s)$ with "y_p" as the output. Suppose*

i) A_k is strictly Hurwitz

ii) There exists an $(n_k + 3) \times (n_k + 3)$ matrix $P_z = P_z^T > 0$ such that

$$A_z^T P_z + P_z A_z = -Q_z \equiv -diag(L_k^T L_k, 0_3)$$

where L_k is a $3 \times n$ matrix such that (L_k, A_k) is observable, and $L_k(sI - A_k)^{-1}B_k$ has no transmission zeros in $Re[s] \geq 0$

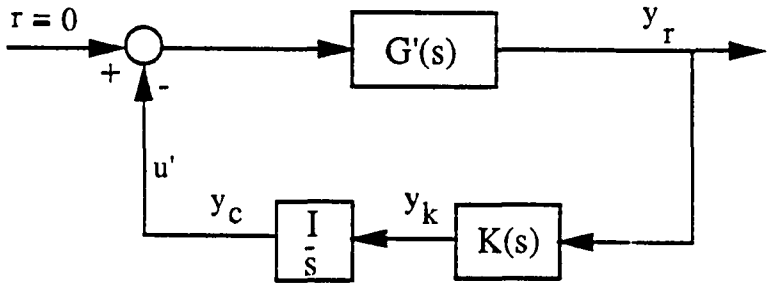

Fig. 3.9 Feedback configuration

iii) $C_z = B_z^T P_z$

iv) $K(s) = C_k(sI - A_k)^{-1}B_k + D_k$ *has no transmission zeros at the origin Then the controller* K *stabilizes* G.

Proof 3.2 *The detailed proof is given in [15].*

The s-domain equivalence of the above theorem is also given in [15] which essentially states that, $K(s)$ *stabilizes* $G(s)$ *if* $K(s)$ *has no transmission zeros at* $s = 0$, *and* $K(s)/s$ *is strongly positive-real* (see [15] for a definition). Many times this condition is simpler to check than its equivalent state-space conditions. For example, if $K(s)$ is given by

$$K_(s) = k\frac{s^2 + \beta_1 s + \beta_0}{s^2 + \alpha_1 s + \alpha_0} \tag{3.22}$$

then, $K(s)/s$ is strongly PR [15] iff $k, \alpha_0, \alpha_1, \beta_0, \beta_1$ are positive, and

$$\alpha_1 \ - \ \beta_1 > 0 \tag{3.23}$$

$$\alpha_1\beta_0 \ - \ \alpha_0\beta_1 > 0 \tag{3.24}$$

Also, in [15] it was shown that $K(s)/s$ can be realized as a strictly proper controller, wherein both position and rate measurements are utilized, by using the following theorem.

Theorem 3.3 *The plant* $G(s)$ *is stabilized by the controller* K' *given by:*

$$\dot{x}_k = A_k x_k + \begin{bmatrix} B_k - A_k L & L \end{bmatrix} \begin{bmatrix} y_p \\ y_r \end{bmatrix} \tag{3.25}$$

$$u_k = C_k x_k \tag{3.26}$$

where L *is a solution of:*

$$D_k - C_k L = 0 \tag{3.27}$$

Proof 3.3 *Refer to [15].*

Dissipative controllers offer a powerful method for robustly stabilizing linear single-body flexible systems. In the next two chapters it will be shown that, the theory of dissipative controllers can be extended to nonlinear multibody systems as well. This chapter will be concluded by some remarks on the passivity of nonlinear systems.

3.5 Passivity in Multibody Nonlinear Systems

The concepts of dissipativity and passivity can be extended to the nonlinear systems as well. The asymptotic stability of interconnected passive systems has been studied in the literature by several authors (see [1] , [40], [16]) from operator theoretic point of view or from the state-space perspective (see [12], [13], [18]- [21]). In particular, in [18]- [21] number of important results were developed for passive systems based on suitable observability hypothesis. Recently, in [41] some of the stricter conditions used in the hypothesis in [18]- [21] were weakened and some generalizations were done. The aim of this section is to establish the passivity of the nonlinear, multibody, flexible systems, modeled by Eq. 2.40, so that, the stability theorems given earlier in this chapter for LTI systems can be extended to these systems.

Consider a closed-loop system shown in Fig. 3.10. P is the nonlinear system under consideration and K is the controller in the feedback loop. r is the reference input and u is the control input to the plant. Then, u can be expressed as

$$u = r - v \tag{3.28}$$

Taking truncated inner product of both the sides with y yields

$$< y, u >_T = < y, r >_T - < y, v >_T \tag{3.29}$$

Rearranging

$$< y, r >_T = < y, u >_T + < y, v >_T \tag{3.30}$$

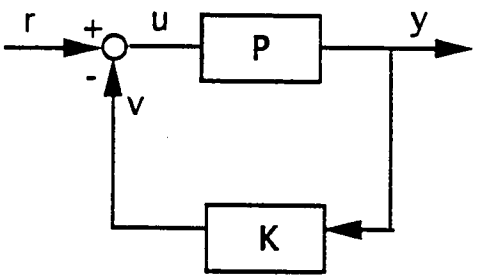

Fig. 3.10 Closed-loop system

Now, if K is strictly passive (i.e. $< y, v >_T > \epsilon \|y\|_T^2 for some \epsilon > 0$), and if P is simply passive (i.e. $< y, u >_T \geq 0$), then $< y, r >_T \geq \|y\|_T^2 \Rightarrow \|y\|_T \|r\|_T \geq \epsilon \|y\|_T^2 \Rightarrow \|y\| \leq \epsilon^{-1} \|r\|_T \Rightarrow$ BIBO stable and closed-loop system is passive. This means that, if for some supply rate $< y, r >_T$ system P is dissipative then any strictly passive controller can stabilize the closed-loop system.

3.5.1 Passivity of Nonlinear, Multibody, Flexible Systems

Consider a system represented by Eq. 2.40. Assuming that all rigid degrees of freedom have associated with them a pair of collocated actuator/sensor, the vector of applied forces, F, is given by $F = B^T u$, where, B is the influence matrix of the control input u and has the form

$$B = [I_{k \times k} \quad 0_{k \times (n-k)}] \tag{3.31}$$

The stiffness and damping matrices K and D have the form,

$$K = \begin{bmatrix} 0_{k \times k} & 0_{k \times (n-k)} \\ 0_{(n-k) \times k} & \overline{K}_{(n-k) \times (n-k)} \end{bmatrix}, \qquad D = \begin{bmatrix} 0_{k \times k} & 0_{k \times (n-k)} \\ 0_{(n-k) \times k} & \overline{D}_{(n-k) \times (n-k)} \end{bmatrix} \tag{3.32}$$

where $\overline{K}$ and $\overline{D}$ are the flexural stiffness and damping matrices associated with the structural members, and the subscripts indicate submatrix dimensions.

Consider the storage function V as

$$V = \frac{1}{2} \dot{p}^T M(p) \dot{p} + \frac{1}{2} p^T (K + K_p) p \tag{3.33}$$

where, K_p has the form

$$K_p = \begin{bmatrix} \overline{K}_{p_{k \times k}} & 0_{k \times (n-k)} \\ 0_{(n-k) \times k} & 0_{(n-k) \times (n-k)} \end{bmatrix}$$

The submatrix $\overline{K}_p$ is symmetric positive definite, so that the sum $(K + K_p)$ is symmetric positive definite matrix. Taking the time derivative of V and using Eq. 2.40 yields

$$\dot{V} = \dot{p}^T [B^T u - C\dot{p} - D\dot{p} - Kp] + \frac{1}{2} \dot{p}^T \dot{M} \dot{p} + \dot{p}^T (K + K_p) p \tag{3.34}$$

Using the property given in theorem 3.1, Eq. 3.32, and after several cancellations

$$\dot{V} = \dot{p}^T u - \dot{q}^T \overline{D} \dot{q} + \dot{\theta}^T \overline{K}_p \theta \tag{3.35}$$

Now if u is selected as

$$u = r - \overline{K}_p \theta$$

then

$$\dot{V} = \dot{p}^T r - \dot{q}^T \overline{D} \dot{q} \tag{3.36}$$

Again, using the argument that $V \geq 0$ implies

$$\int_0^T \dot{V} dt \geq 0$$

Substituting for $\dot{V}$

$$0 \leq \int_0^T \dot{q}^T r - \dot{q}^T \overline{D} q dt \tag{3.37}$$

$$\Rightarrow \int_0^T \dot{q}^T \overline{D} q dt \leq \int_0^T \dot{p}^T r dt \Rightarrow < \dot{p}, r >_T \geq 0 \tag{3.38}$$

This means that, the system is passive for supply rate $< \dot{p}, r >_T$ with storage function $V = \frac{1}{2}\dot{p}^T M(p)\dot{p} + \frac{1}{2}p^T(K + K_p)p$. The next two chapters are devoted to the theoretical development of the stability results by exploiting this passivity property of the system.

Chapter 4

STATIC DISSIPATIVE CONTROLLERS (SDC)

4.1 Introduction

In this chapter it is proved that the stability properties derived for the linear time-invariant non-articulated flexible structures under dissipative compensation can be extended to the nonlinear, multibody flexible structures as well. The approach here is to use the mathematical model developed in Chapter 2, which is in a general form, to represent the multibody, nonlinear, flexible space systems. The organization of this chapter is as follows. In the first section the global asymptotic stability of static dissipative controllers has been established for the perfect actuators and sensors. Then, the results are extended to show the robustness of stability properties to certain realistic actuator/sensor nonlinearities. The effects of dead-zone nonlinearity in the actuators are also investigated.

4.2 Static Dissipative Controllers with Perfect Actuators/Sensors

Recall the mathematical model of flexible multibody space structures given by 2.40:

$$M(p)\ddot{p} + C(p,\dot{p})\dot{p} + D\dot{p} + Kp = B^T u \tag{4.1}$$

where $\{p\} = \{\theta^T, q^T\}^T$, θ is the k-vector of rigid body coordinates and q is the $(n-k)$ vector of the flexural coordinates. $M(p) = M^T(p) > 0$ is the configuration-dependent mass-inertia matrix; $C(p,\dot{p})$ corresponds to Coriolis and centrifugal forces; D is the symmetric, positive semidefinite damping matrix; K is the symmetric, positive semidefinite stiffness matrix; and u is the k vector of applied torques. B is the influence matrix of the control input u and has the form $B = [I_{k\times k} \quad 0_{k\times(n-k)}]$. It should be noted that such systems always have zero-frequency modes associated with rigid-body coordinates.

Consider the static dissipative control law u, given by:

$$u = -G_p y_p - G_r y_r \tag{4.2}$$

where

$$y_p = Bp \qquad and \qquad y_r = B\dot{p} \tag{4.3}$$

y_p and y_r are measured angular position and rate vectors.

Theorem 4.1 *Suppose G_p and G_r are symmetric and positive definite. Then, the closed-loop system given by equations 4.1 and 4.2 is globally asymptotically stable.*

Proof 4.1 *Consider the Lyapunov function*

$$V = \frac{1}{2}\dot{p}^T M(p)\dot{p} + \frac{1}{2}p^T(K + B^T G_p B)p \tag{4.4}$$

V is clearly positive definite since $M(p)$ and $(K + B^T G_p B)$ are positive definite symmetric matrices. Taking the time derivative and letting $\overline{K} = (K + B^T G_p B)$,

$$\dot{V} = \dot{p}^T M\ddot{p} + \frac{1}{2}\dot{p}^T \dot{M}\dot{p} + \dot{p}^T \overline{K} p \tag{4.5}$$

Using 4.1 in 4.5, get,

$$\dot{V} = \dot{p}^T[B^T u - C\dot{p} - D\dot{p} - Kp] + \frac{1}{2}\dot{p}^T \dot{M}\dot{p} + \dot{p}^T \overline{K} p \tag{4.6}$$

Now substituting 4.1 and 4.2 in 4.6,

$$\dot{V} = \dot{p}^T B^T(-G_p\theta - G_r\dot{\theta}) + \dot{p}^T(\frac{1}{2}\dot{M} - C) \quad \dot{p} - \dot{p}^T D\dot{p} - \dot{p}^T Kp + \dot{p}^T \overline{K}p \tag{4.7}$$

$$\dot{V} = \dot{p}^T(\frac{1}{2}\dot{M} - C)\dot{p} - \dot{p}^T \overline{K}p + \dot{p}^T \overline{K}p - \dot{p}^T(D + B^T G_r B)\dot{p} \tag{4.8}$$

Now, using a very important property of the system, that $(\frac{1}{2}\dot{M} - C)$ *is a skew symmetric matrix, Eq. 2.42, which is the characteristic of the systems whose dynamical equations of motion have the same form as Eq. 4.1, yields,* $\dot{p}^T(\frac{1}{2}\dot{M} - C)\dot{p} = 0$ *and, after some cancellations, obtain*

$$\dot{V} = -\dot{p}^T(D + B^T G_r B)\dot{p} \tag{4.9}$$

Since $(D + B^T G_r B)$ *is the positive definite symmetric matrix,*

$$\dot{V} \leq 0 \tag{4.10}$$

i.e., $\dot{V}$ *is negative semidefinite in* p *and* $\dot{p}$ *and*

$$\dot{V} = 0 \Rightarrow \dot{p} = 0 \Rightarrow \ddot{p} = 0 \tag{4.11}$$

Substituting in the closed-loop equation, get

$$(K + B^T G_p B)p = 0 \qquad \Rightarrow p = 0 \tag{4.12}$$

Thus, $\dot{V}$ *is not zero along any trajectories; then, by LaSalle's theorem, the system is globally asymptotically stable.*

The significance of this result is that *any nonlinear multibody system in this class can be robustly stabilized with this control law.* In the case of manipulators, this means that one can accomplish any terminal position from any initial position with *guaranteed asymptotic stability.*

4.3 Robustness to Actuator/Sensor Nonlinearities

Although, as shown in the proof of theorem 4.1, the static dissipative controller 4.2 globally asymptotically stabilizes the nonlinear system 4.1 in the presence of perfect (i.e., linear, instantaneous) actuators and sensors, in practice, these devices have nonlinearities and phase lags. Therefore, for practical applications, the controller 4.2 should be robust to the nonlinearities and the phase shifts in the actuator/sensor. In Chapter 2, different types of realistic nonlinearities present in the actuating and sensing devices are given. The following theorem extends the results of section 3.4.2 to the case of nonlinear flexible multibody systems. That is, the robust stability property of the static dissipative controllers is proved in the presence of a wide class of actuator/sensor nonlinearities. In particular, it is proved that the static dissipative controller preserves global asymptotic stability when actuators have monotonically increasing nonlinearities and sensors have nonlinearities that belong to the $(0, \infty)$ sector 3.4.2.

In the presence of actuator/sensor nonlinearities, the actual input is given by:

$$u = \psi_a[-G_p\psi_p(y_p) - G_r\psi_r(y_r)] \tag{4.13}$$

where ψ_a, ψ_p, and ψ_r denote the actuator nonlinearity and the position and rate sensor nonlinearities, respectively. Assuming G_p and G_r are diagonal,

$$u_i = \psi_{ai}[-G_{pi}\psi_{pi}(y_{pi}) - G_{ri}\psi_{ri}(y_{ri})] \tag{4.14}$$

It is assumed that ψ_{ai}, ψ_{pi}, and ψ_{ri} $(i = 1, 2, ..., k)$ are continuous single-valued functions: $\mathbf{R} \rightarrow \mathbf{R}$. The following theorem gives the sufficient conditions for stability.

Theorem 4.2 *Consider the closed-loop system given by 4.1, 4.2, 4.3, and 4.13, where G_p and G_r are diagonal with positive entries. Suppose ψ_{ai}, ψ_{pi}, and ψ_{ri} are single-valued, time invariant continuous functions, and that, for $i = 1, 2, ..., k$,*

(i)$\psi_{ai}(0) = 0$, ψ_{ai} are monotonically increasing (Fig. 3.7) and belong to $(0, \infty)$ sector.
(ii)ψ_{pi}, ψ_{ri} belong to the $(0, \infty)$ sector(Fig. 3.8).
Then, the closed-loop system is globally asymptotically stable.

Proof 4.2 *Let $w = -y_p = -\theta$ (k-vector). Define*

$$\overline{\psi}_{pi}(\nu) = -\psi_{pi}(-\nu) \tag{4.15}$$

$$\overline{\psi}_{ri}(\nu) = -\psi_{ri}(-\nu) \tag{4.16}$$

If ψ_{pi}, ψ_{ri} $\epsilon(0, \infty)$ or $[0, \infty)$ sector then $\overline{\psi}_{pi}$, $\overline{\psi}_{ri}$ also belong to the same sector. Now, consider the following Luré-Postnikov Lyapunov function :

$$V = \frac{1}{2}\dot{p}^T M(p)\dot{p} + \frac{1}{2}q^T\overline{\overline{K}}q + \sum_{i=1}^{k}\int_0^{w_i}\psi_{ai}\{G_{pi}\overline{\psi}_{pi}(\nu)\}d\nu \tag{4.17}$$

where, $\overline{\overline{K}}$ is the symmetric positive definite part of K. Taking the time derivative and using Eq. 4.1,

$$\dot{V} = \dot{p}^T[B^T u - C\dot{p} - D\dot{p} - Kp] + \frac{1}{2}\dot{p}^T\dot{M}\dot{p} \tag{4.18}$$

$$+\sum_{i=1}^{k}\dot{w}_i\psi_{ai}\{G_{pi}\overline{\psi}_{pi}(w_i)\} + \dot{q}^T\overline{\overline{K}}q \tag{4.19}$$

Upon several cancellations and using the "skew symmetric" property of $(\frac{1}{2}\dot{M} - C)$,

$$\dot{V} = \sum_{i=1}^{k}u_i\dot{\theta}_i - \dot{q}^T\overline{D}\dot{q} + \sum_{i=1}^{k}\dot{w}_i\psi_{ai}\{G_{pi}\overline{\psi}_{pi}(w_i)\} \tag{4.20}$$

where, matrix $\overline{D}$ is the positive definite part of D.

$$\dot{V} = -\dot{q}^T\overline{D}\dot{q} - \sum_{i=1}^{k}\dot{w}_i(\psi_{ai}[G_{ri}\overline{\psi}_{ri}(\dot{w}_i) + G_{pi}\overline{\psi}_{pi}(w_i)] \tag{4.21}$$

$$-\psi_{ai}[G_{pi}\overline{\psi}_{pi}(w_i)]) \tag{4.22}$$

If ψ_{ai} are monotonic nondecreasing and ψ_{ri} belong to the $(0, \infty)$ sector, $\dot{V} \leq 0$, and it can be concluded that the system is at least Lyapunov-stable. Now it will be proved that, in fact, the system is globally asymptotically stable. From Eq. 4.22, $\dot{V} \leq -\dot{q}^T\overline{D}\dot{q}$,

and $\dot{V} = 0$ *only when* $\dot{q} = 0$ *and* $\dot{w} = 0$, *which implies* $\dot{\theta} = 0 \Rightarrow \dot{p} = 0 \Rightarrow \ddot{p} = 0$. *Substituting in the closed-loop equation,*

$$Kp = B^T \psi_a[-G_p \psi_p(\theta)] \tag{4.23}$$

$$\begin{bmatrix} 0 \\ \overline{\overline{K}}q \end{bmatrix} = \begin{bmatrix} \psi_a\{-G_p \psi_p(y_p)\} \\ 0 \end{bmatrix} \tag{4.24}$$

$$\Rightarrow \psi_a[-G_p \psi_p(\theta)] = 0, \qquad and \qquad q = 0 \tag{4.25}$$

If ψ_{ai} *and* ψ_{pi} *belong to the* $(0, \infty)$ *sector,* $\psi_{ai}(\nu) = \psi_{pi}(\nu) = 0$ *only when* $\nu = 0$. *Therefore,* $\theta = 0$. *Thus,* $\dot{V} = 0$ *only at the origin, and the system is globally asymptotically stable.*

4.3.1 Effect of Saturation Nonlinearity

In the case when actuator nonlinearities are of the monotonic nondecreasing rather than increasing type (such as saturation nonlinearity), $\dot{V}$ can be 0 even if $\dot{w} \neq 0$. However, it will be shown that every system trajectory along which $\dot{V} \equiv 0$, has to go to the origin asymptotically. When $\dot{w} \neq 0$, $\dot{V} \equiv 0$ only when all actuators are saturated. Then, from the equations of motion, it means that system trajectories will go unbounded which is not possible since we have already proved that the system is Lyapunov-stable. Hence, system trajectories have to approach the origin asymptotically and again the system is globally asymptotically stable.

4.4 Region of Ultimate Boundedness in The Presence of Actuator Dead-zone Nonlinearity

In the previous section global asymptotic stability of nonlinear multibody flexible space-structures under static dissipative compensation was established. Furthermore, the stability was shown to be robust to certain actuator and sensor nonlinearities, modeling errors, and parametric uncertainty. In particular, it was proved that the static dissipative controller preserves global asymptotic stability when actuators have

monotonically increasing nonlinearities and sensors have nonlinearities that belong to the $(0, \infty)$ sector. Although the saturation type actuator nonlinearity was allowed under the assumptions of the theorem, another realistic nonlinearity such as dead-zone nonlinearity was not allowed. In this section, the effects of dead-zone nonlinearity on the stability of the system are studied.

4.4.1 Region of Ultimate Boundedness:

In the presence of deadzone in the actuator nonlinearity system under consideration will not have asymptotically stable origin, but will instead have the property of ultimate boundedness; i.e. for all initial conditions, solutions ultimately enter a compact region containing the origin in finite time, and remain in the region thereafter. Estimates of the extent of this region will be found by means of Lyapunov functions. A system under consideration, as given in Eq. 4.1, is:

$$M(p)\ddot{p} + C(p,\dot{p})\dot{p} + D\dot{p} + Kp = B^T u \tag{4.26}$$

The control law considered is, the static dissipative control law u, given by:

$$u = -G_p y_p - G_r y_r \tag{4.27}$$

where,

$$y_p = Bp \qquad and \qquad y_r = B\dot{p} \tag{4.28}$$

y_p and y_r are measured angular position and rate vectors. In the presence of actuator/sensor nonlinearities, recall that, the actual input is given by:

$$u = \psi_a[-G_p\psi_p(y_p) - G_r\psi_r(y_r)] \tag{4.29}$$

where ψ_a, ψ_p, and ψ_r denote the actuator nonlinearity and the position and rate sensor nonlinearities, respectively. Assuming G_p and G_r are diagonal,

$$u_i = \psi_{ai}[-G_{pi}\psi_{pi}(y_{pi}) - G_{ri}\psi_{ri}(y_{ri})] \tag{4.30}$$

It was also assumed that ψ_{ai}, ψ_{pi}, and ψ_{ri} $(i = 1, 2, ..., k)$ are continuous single-valued functions: $\mathbf{R} \rightarrow \mathbf{R}$. Then, theorem 4.2 gives the sufficient conditions for stability.

In the presence of deadzone, the condition (i) of theorem 4.2 is violated and asymptotic stability can not be guaranteed. In order to show that the system has a region of ultimate boundedness in the presence of deadzone in the actuators, we require the following definition and theorem taken from [42], with minor modifications:

Definition: The system 4.1 is ultimately bounded in a compact region R if there exists a t_1 such that, for all $x(t_0)$, $x(t) \epsilon R$, $\forall\, t \geq t_1 \geq t_0$.

Theorem 4.3 *(Ref. to [42]) Let R be a compact region containing the origin, defined by $V(x) \leq \gamma$, where $V(x)$ is a scalar function with continuous partial derivatives and the properties that*

$$
\begin{aligned}
&(i) \qquad V(x) > 0 \quad x \epsilon R^c \\
&(ii) \qquad V(x) \rightarrow \infty \quad as \quad |x| \rightarrow \infty \\
&(iii) \qquad -\dot{V}(x) > 0 \quad x \epsilon R^c
\end{aligned}
$$

where R^c is the complement of R. Then 4.1 is ultimately bounded in R.

The Lyapunov function for system 4.1, used in the proof of theorem 4.2, is given by

$$V = \frac{1}{2}\dot{p}^T M(p)\dot{p} + \frac{1}{2}q^T \overline{\overline{K}} q + \sum_{i=1}^{k} \int_0^{w_i} \psi_{ai}\{G_{pi}\overline{\psi}_{pi}(\nu)\}d\nu \tag{4.31}$$

and, its time derivative along the trajectories of the system is

$$\dot{V} = -\dot{q}^T \overline{D}\dot{q} - \sum_{i=1}^{k} \dot{w}_i(\psi_{ai}[G_{ri}\overline{\psi}_{ri}(\dot{w}_i) + G_{pi}\overline{\psi}_{pi}(w_i)] - \psi_{ai}[G_{pi}\overline{\psi}_{pi}(w_i)]) \tag{4.32}$$

Let the actuator nonlinearity $\psi_{ai}(\nu)$ has deadzone in the region $|\nu| < d$. Then, from 4.31 and 4.32 it can be seen that V is no more positive definite (p.d.) in p and $\dot{p}$, and $\dot{V}$ is no more negative definite (n.d.) in $\dot{p}$. Now, the aim is to find the region $\mathcal{R}^c$ in which V will be p.d. and $\dot{V}$ will be n.d. at least along the trajectories of the system. Then, the complement of $\mathcal{R}^c$, $\mathcal{R}$, will be the required region of ultimate boundedness.

Let us define

$$\Phi_{pi}(w_i) = G_{pi}\overline{\psi}_{pi}(w_i) \qquad i = 1, 2, ..k. \tag{4.33}$$

and

$$x = \{p, \dot{p}\}^T.$$

Then, the most conservative estimate of the region $\mathcal{R}$ can be found as follows.

Consider a region

$$\Omega = \{x \epsilon R^n | \Phi_{pi} \leq d \quad for \quad i = 1, 2, ..k\} \tag{4.34}$$

Then, the required region $\mathcal{R}$ is given by

$$\mathcal{R} = \{x \epsilon R^n | V(x) \leq \gamma\} \tag{4.35}$$

where

$$\gamma = \max_{x \epsilon \Omega} V(x).$$

Now it can be seen that, in $\mathcal{R}^c$ $\dot{V}(x)$ is negative and $V(x)$ is positive along the nonzero trajectories of the system.

An estimate of the region of ultimate boundedness can be obtained in this manner. However, the computational methods to determine it remains a problem for future studies.

4.5 Remarks

It is proved that, under static dissipative control, nonlinear, multibody, flexible space structures exhibit global asymptotic stability. The stability is not only robust to the modeling errors and parametric uncertainties, but also to a wide class of nonlinearities in the actuators and sensors. This has a significant practical value since the mathematical models of the system usually have substantial inaccuracies, and the actuation and sensing devices available are not perfect. It is also shown that in the case of deadzone type actuator nonlinearity, although the system trajectories do not go to the equilibrium state asymptotically, they remain ultimately bounded in a compact region in the neighborhood of a equilibrium point. The next chapter extends some of the results of this chapter to a more versatile class of dissipative controllers, called dynamic dissipative controllers.

Chapter 5

DYNAMIC DISSIPATIVE CONTROLLERS (DDC)

5.1 Introduction

In this chapter, stability characteristics of dynamic dissipative controllers are investigated for multibody flexible space structures. The problem addressed is that of proving asymptotic stability of dynamic dissipative controllers. The stability proof uses the Lyapunov approach and exploits the inherent passivity of such systems. For such systems these controllers are shown to be robust to parametric uncertainties and unmodeled dynamics. The results are applicable to a large class of structures including flexible space structures with articulated flexible appendages.

In Chapter 4, it was shown that the static dissipative controllers are not only robust to parametric uncertainties and unmodeled dynamics but also to a wide range of actuator/sensor nonlinearities. This chapter is aimed at extending the results of Chapter 4, from static dissipative controllers to include a more versatile class of controllers known as dynamic dissipative controllers. The work of this chapter can also be considered as an extension of the stability results obtained for the linear case, noted in Chapter 3, to the nonlinear case. The stability proof given here uses Lyapunov approach along with LaSalle's theorem and is based on Chapter 4. The Lyapunov

function used is an energy type quadratic function augmented with an appropriate positive definite function to prove global asymptotic stability. The stability proof by Lyapunov's method can take a simpler form if the Work-Energy Rate principle [11] is used. However, since the Work-Energy Rate principle is applicable only when the system is holonomic and scleronomic in nature, the more general approach of direct substitution of the equations of motion was employed in evaluating the time derivative of the Lyapunov function. Also, in [11], the virtual spring-mass-damper approach was taken to design the controller consisting of a second-order passive system which can be considered as a special class of the more general dynamic dissipative controllers considered in this chapter.

5.2 Dynamic Dissipative Controllers

Rewriting the mathematical model 3.33 of flexible multibody space structures for convenience,

$$M(p)\ddot{p} + C(p,\dot{p})\dot{p} + D\dot{p} + Kp = B^T u \tag{5.1}$$

where $\{p\} = \{\theta^T, q^T\}^T$, θ is an r-vector of rigid body coordinates and q is an $(n-r)$ vector of the flexural coordinates. $M(p)$ is the configuration dependent mass-inertia matrix; $C(p,\dot{p})$ corresponds to Coriolis and centrifugal forces; D is the damping matrix; K is the stiffness matrix; and u is the vector of applied torques. The matrices $M(p)$ and $C(p,\dot{p})$ have coupling terms between θ and q. It is assumed that each of the rigid body coordinates has an associated collocated actuator/sensor pair and that each actuator produces an external input going into the associated rigid-body coordinate only. Then, the input matrix B^T has the form,

$$B^T = \begin{bmatrix} I_{r\times r} \\ 0_{(n-r)\times r} \end{bmatrix}.$$

Consider the system given by Eq. 5.1. Each of the collocated sensors measures only the relative rigid rotation between the two members. Let y_p and y_r denote

the measured angular position and rate vectors. Then, the output equations take the form,

$$y_p = Bp \qquad and \qquad y_r = B\dot{p} \tag{5.2}$$

Now consider the configuration of Fig. 5.1. Suppose a controller $\mathcal{K}(s)$ is represented by the minimal realization:

$$\dot{x}_k = A_k x_k + B_k u_k \tag{5.3}$$

$$y_k = C_k x_k + D_k u_k \tag{5.4}$$

Define

$$\dot{v} = y_k \tag{5.5}$$

$$z = (x_k^T, v^T)^T \tag{5.6}$$

$$y_c = v \tag{5.7}$$

Equations 5.3- 5.7 can be combined as:

$$\dot{z} = A_z z + B_z u_k \tag{5.8}$$

$$y_c = C_z z \tag{5.9}$$

where

$$A_z = \begin{bmatrix} A_k & 0 \\ C_k & 0 \end{bmatrix} \quad B_z = \begin{bmatrix} B_k \\ D_k \end{bmatrix} \quad C_z = \begin{bmatrix} 0 & I_r \end{bmatrix} \tag{5.10}$$

Theorem 5.1 *Consider a nonlinear plant 5.1 with "y_p" as the output. Suppose*

i) A_k is strictly Hurwitz

ii) There exists an $(n_k + r) \times (n_k + r)$ matrix $P_z = P_z^T > 0$ such that

$$A_z^T P_z + P_z A_z = -Q_z \equiv -diag(L_k^T L_k, 0_r) \tag{5.11}$$

where L_k is an $r \times n$ matrix such that (L_k, A_k) is observable, and $L_k(sI - A_k)^{-1}B_k$ has no transmission zeros in $Re[s] \geq 0$

$$iii) \quad C_z = B_z^T P_z \tag{5.12}$$

iv) $\mathcal{K}(s) = C_k(sI - A_k)^{-1}B_k + D_k$ has no transmission zeros at the origin.

Then the closed-loop system given by equations 5.1, 5.2, 5.8, and 5.9 is globally asymptotically stable.

Proof 5.1 *Consider the Lyapunov function,*

$$V = \frac{1}{2}\dot{p}M(p)\dot{p} + \frac{1}{2}q^T\overline{K}q + \frac{1}{2}z^T P_z z \tag{5.13}$$

where $\overline{K}$ is the symmetric positive definite part of K (i.e., the part associated with nonzero stiffness). Then

$$\dot{V} = \dot{p}M(p)\ddot{p} + \frac{1}{2}\dot{p}^T\dot{M}\dot{p} + \dot{q}^T\overline{K}q + \frac{1}{2}(\dot{z}^T P_z z + z^T P_z \dot{z}) \tag{5.14}$$

which after substituting for $M(p)\ddot{p}$ using 5.1, and for $\dot{z}$ using 5.8, 5.14 becomes:

$$\begin{aligned}\dot{V} = \dot{p}^T B^T u - \dot{q}^T\overline{D}\dot{q} + \dot{p}^T(\frac{1}{2}\dot{M} - C)\dot{p} - \dot{p}^T K p \\ + \dot{q}^T\overline{K}q + \frac{1}{2}[(z^T A_z^T + u_k^T B_z^T)P_z z + \\ z^T P_z(A_z z + B_z u_k)]\end{aligned} \tag{5.15}$$

An important property for systems, whose dynamic equations are of the form 5.1, is that the matrix $(\frac{1}{2}\dot{M} - C)$ is skew symmetric 2.42. This property is exploited to recognize that $\dot{p}^T(\frac{1}{2}\dot{M} - C)\dot{p} = 0$.

$$\begin{aligned}\dot{V} = \dot{p}^T B^T u - \dot{q}^T\overline{D}\dot{q} + \frac{1}{2}z^T(A_z^T P_z + + P_z A_z)z \\ + \frac{1}{2}u_k^T(B_z^T P_z)z + \frac{1}{2}z^T(P_z B_z)u_k\end{aligned} \tag{5.16}$$

$$\dot{V} = -\dot{q}^T\overline{D}\dot{q} + \dot{p}^T B^T u - \frac{1}{2}z^T Q_z z + z^T C_z^T u_k \tag{5.17}$$

$$\dot{V} = -\dot{q}^T\overline{D}\dot{q} - \frac{1}{2}z^T Q_z z - u_k^T y_c + y_c^T u_k \tag{5.18}$$

Noting (Fig. 5.1) that $u = -y_c = -C_z z$ *and* $B\dot{p} = y_r = u_k$,

$$\dot{V} = -\dot{q}^T \overline{D} \dot{q} - \frac{1}{2} z^T Q_z z \tag{5.19}$$

Since $\overline{D}$ *and* Q_z *are positive definite, it follows that* $\dot{V} \leq 0$, *i.e.,* $\dot{V}$ *is negative semidefinite in* p, $\dot{p}$, *and* z. *Now* $\dot{V} = 0$ *only if* $\dot{q} = 0$ *and* $L_k x_k = 0$. *Since* (A_k, B_k, L_k) *has no transmission zeros in* $Re(s) \geq 0$ *and* (A_k, L_k) *is observable, this requires that* $y_r \rightarrow 0$ *and* $x_k \rightarrow 0$. *But,* $y_r \rightarrow 0 \Rightarrow \dot{\theta} \rightarrow 0 \Rightarrow \dot{p} \rightarrow 0$ *then, with* $\dot{q} = 0$, *this implies that* $\ddot{p} = 0$. *Substituting in the equation 5.1 get,* $\theta \rightarrow \theta_{ss}$ *and* $q \rightarrow 0$, *where* θ_{ss} *is some steady-state value of* θ. *This only shows that the system is Lyapunov stable.*

Now consider the configuration shown in Fig. 5.2 which is obtained by a nonsingular similarity transformation $\hat{T}$ *given by,*

$$\hat{T} = \begin{bmatrix} I_r & 0 & 0 \\ 0 & A_k & B_k \\ 0 & C_k & D_k \end{bmatrix} \tag{5.20}$$

Clearly, $\hat{T}$ *is nonsingular iff* $\mathcal{K}(s)$ *has no transmission zeros at the origin. The transformed system has controller state equations*

$$\dot{x}_k = A_k x_k + B_k y_p \tag{5.21}$$

$$u = -y_k = -\left(C_k x_k + D_k y_p\right) \tag{5.22}$$

Since transformation $\hat{T}$ *is linear and nonsingular, the transformed system is also Lyapunov-stable like the original system. Now it will be shown that the system is, in fact, asymptotically stable.*

Suppose that the system is not asymptotically stable. Then, referring to Fig. 5.2, suppose the output y_p *reaches some steady-state value, say* $\overline{y}_p$. *Since* $\mathcal{K}(s)$ *is linear time-invariant and has minimal realization 5.3- 5.4, the output* y_k *of the controller will also reach some steady-state* $\overline{y}_k$. *Consequently, the control input* u *will also have some constant value* $\overline{u}$. *From the physical considerations it can be seen*

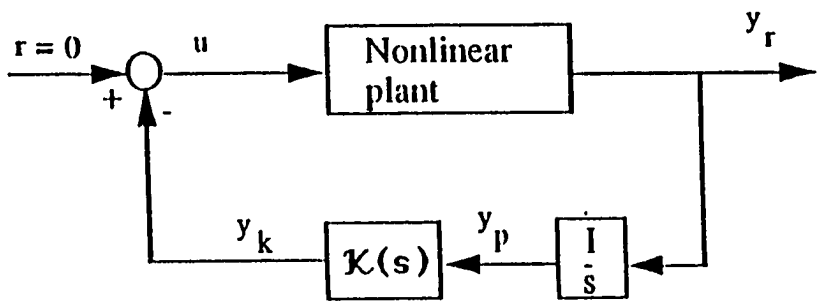

Fig. 5.1 Feedback configuration

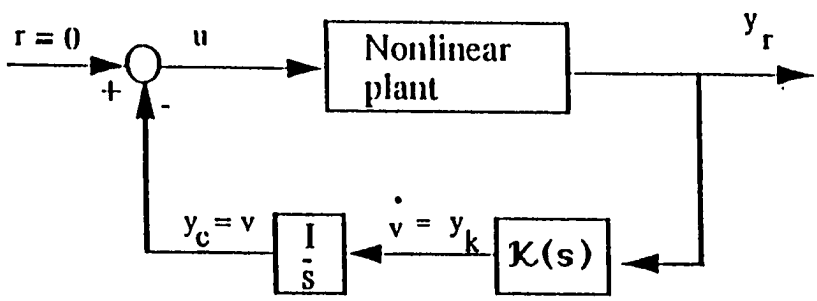

Fig. 5.2 Feedback configuration

that the nonlinear system under consideration has the property that nonzero constant input $\overline{u}$ will produce some nonzero output y_r (this is equivalent to the LTI property of having no zeros at the origin). However, it has already been shown that $y_r \rightarrow 0$; thus $u \rightarrow 0 \Rightarrow y_k \rightarrow 0$ and $\dot{x}_k \rightarrow 0$.

Now, from the controller state equation 5.3,

$$\dot{x}_k = 0 \Rightarrow x_k = -A_k^{-1} B_k y_p \tag{5.23}$$

Substituting in equation 5.4 with $y_k = 0$ yields

$$y_k = 0 = C_k x_k + D_k y_p = (D_k - C_k A_k^{-1} B_k) y_p \tag{5.24}$$

Since $K(s)$ satisfies a minimum phase condition, the matrix in the parenthesis is nonsingular and, therefore, from equation 5.24 $y_p \rightarrow 0$. This proves that the system is asymptotically stable.

Since no assumptions were made as regards to the modeling accuracy as well as parametric variations, the stability is robust to modeling errors and parametric uncertainties.

5.3 Remarks

It is proved that, under dynamic dissipative control, nonlinear multibody flexible space structures exhibit global asymptotic stability. The stability is robust to modeling errors and parametric uncertainties as long as the I/O map from torque inputs to velocity outputs is passive. This result has a significant practical value. It enables a control designer to have more design freedom than is available with static dissipative controllers. Methods for designing such controllers is a challenging task and future work will address methods for controller synthesis.

Chapter 6

NUMERICAL EXAMPLES

The purpose of this chapter is to introduce the example systems used to verify some of the stability results obtained in chapters 4 and 5. The synthesis of static as well as dynamic dissipative controllers for nonlinear systems is still a topic of future research. However, in the example problem, for the static dissipative compensaters, the controller gains are selected based on several trials, since the purpose is to validate (numerically) the stability results derived in chapter 4. The second example problem is the application of dynamic dissipative controllers to the linear systems, which is a special case of nonlinear systems. A systematic procedure can be employed to synthesize the dynamic dissipative controller for linear systems since the performance function is well defined. In the case of nonlinear systems, the performance function can not be well defined which makes the synthesis problem extremely difficult.

6.1 Application of SDC

The example system used for validation of theoretical results is shown in Fig. 6.1. It consists of a central 10-bay, flexible truss with a two-link flexible manipulator at one end. This represents a flexible space-structure with flexible, articulated appendage. It has three pairs of collocated actuators and sensors; each one associated with the rigid degree of freedom. One of the actuator/sensor pairs is located at the center of the truss, and other two are at the joints between truss and arm 1, and arm 1 and arm

2, respectively. All bodies were modeled as flexible and their modal information was obtained using MSC/NASTRAN, a well known finite element commercially available software by Macneal-Schwendler Corporation. The complete nonlinear simulation was done using another commercially available software "DADS" for multibody analysis and design software by Computer Aided Design Software Inc.(CADSI), Oakdale, Iowa. Interested readers can refer to [43] for more information about the software.

6.1.1 Model Description

The example structure has a 100 inches long 10-bay truss with a two-link manipulator at one end. Each of the arms has a length of 50 inches. The central truss has (refer Fig. 6.1) 89 longerons, 40 battens, and 10 diagonals. Each of the arms is modeled with 10 CBAR elements in NASTRAN. The cross section of the arms is circular with 1.0 inch diameter. The material chosen for the arms has a mass density of 4.14e-04 $lb-sec^2/in^4$, modulus of elasticity E=1e+07 lb/in^2, and Poisson's ratio of 0.33. The central truss is of the same material, and each of the truss members were modeled as 0.5in diameter bar elements. As shown in the Fig. 6.1, there are two revolute joints; one between the central truss member and arm 1, and another between arm 1 and arm 2. It is assumed that there are three actuator/sensor pairs, one each at the revolute joints and one at the center of the truss for attitude control. It is also assumed that both position and rate measurements are available. Note that Fig. 6.1 shows the zero position of the system.

6.1.2 Simulation Results

The control problem was set up as follows. The initial configuration of the system was chosen by setting revolute joint 2 at an angle of 1 rad. The objective was to restore the zero state of the system, i.e. the configuration shown in Fig. 6.1. After several trials a static dissipative controller was designed to accomplish the task. As the system starts moving all members start moving relative to one another and there

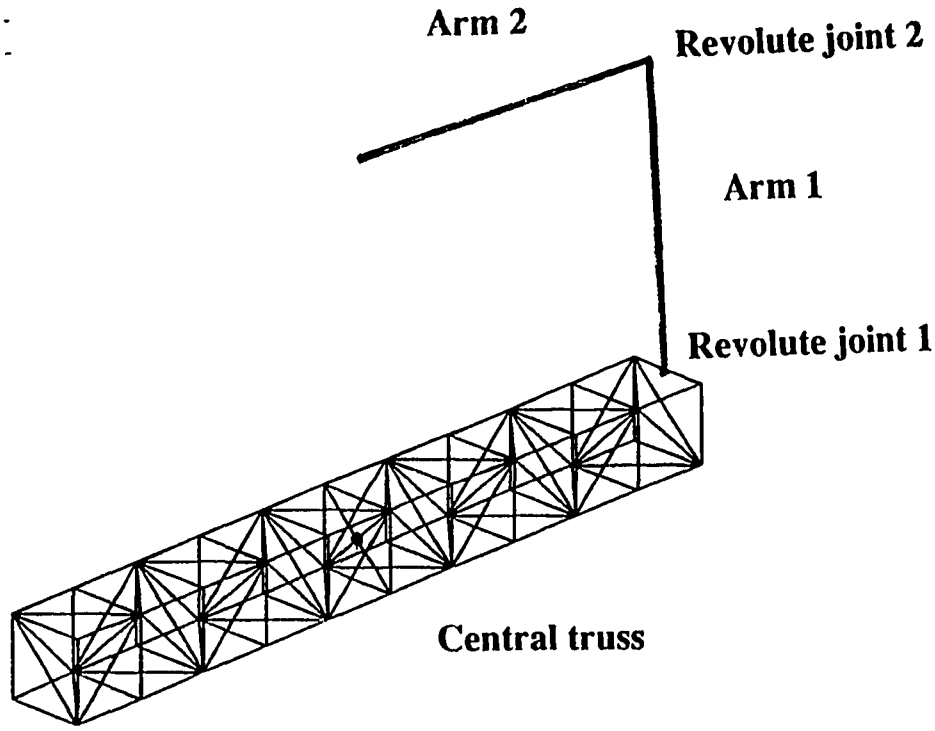

Fig. 6.1 Flexible space-truss with articulated appendage

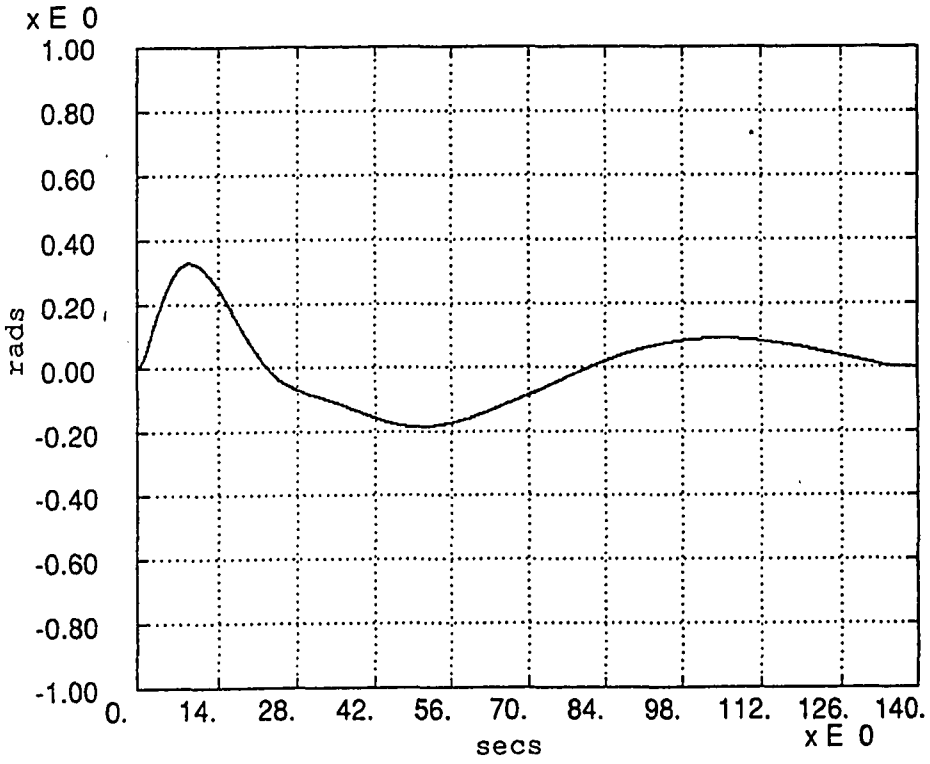

Fig. 6.2 Angular displacement of revolute joint 1.

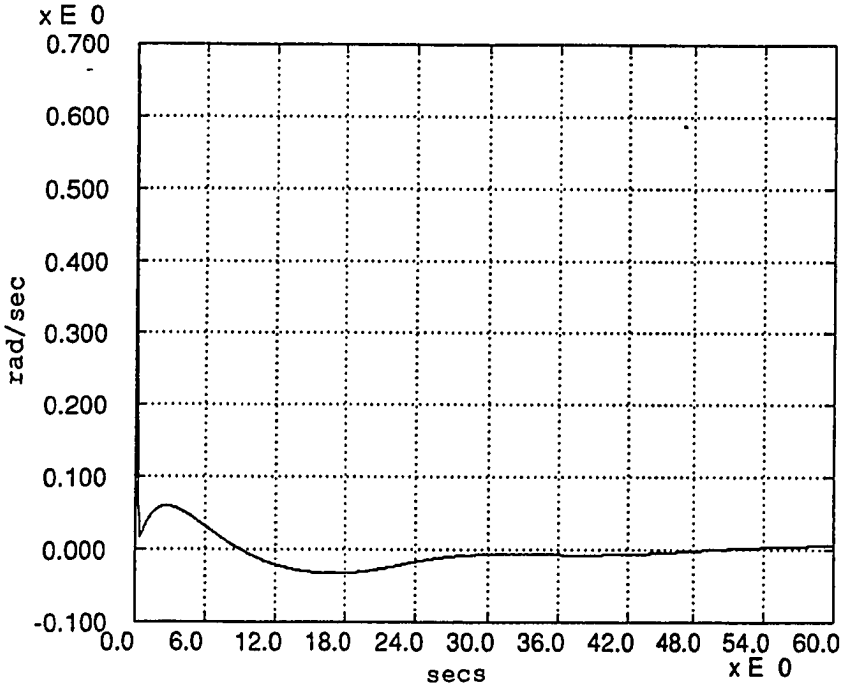

Fig. 6.3 Angular velocity of revolute joint 1.

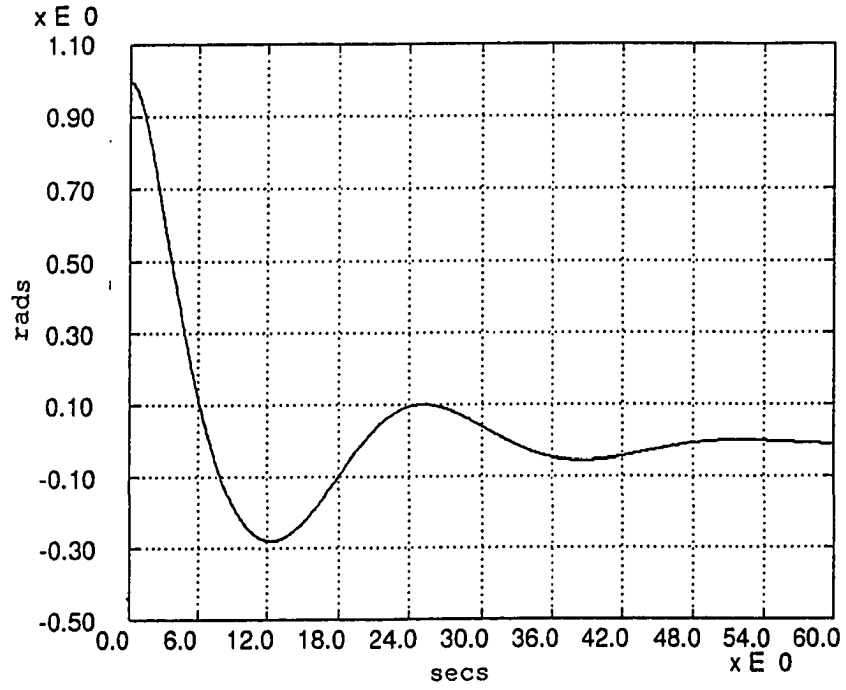

Fig. 6.4 Angular displacement of revolute joint 2.

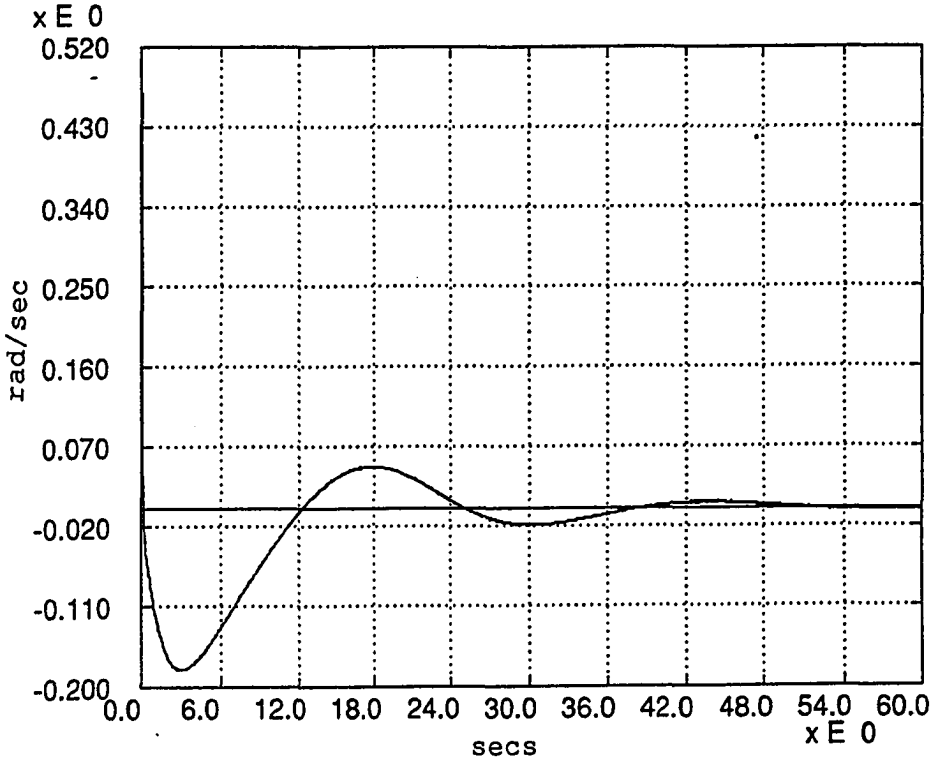

Fig. 6.5 Angular velocity of revolute joint 2.

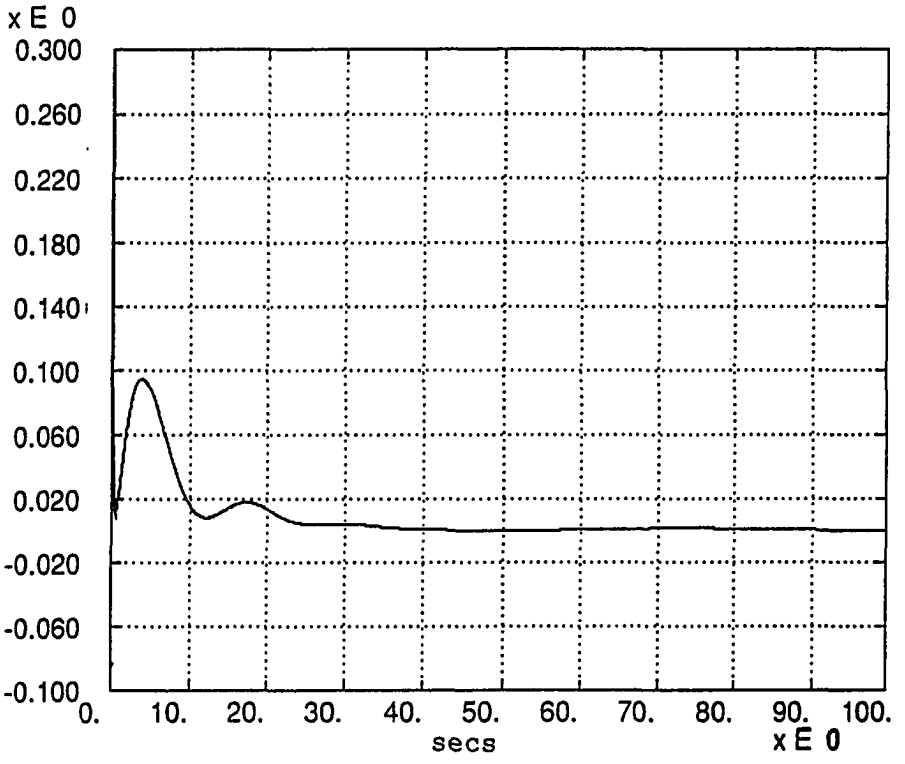

Fig. 6.6 Total energy of the system.

is a dynamic interaction between members. The simulation performed incorporated complete nonlinear and coupling effects. The joint angle and velocity responses for revolute joint 1 are shown Fig. 6.2 and Fig. 6.3, respectively. Similarly, the position and velocity responses for revolute joint 2 are shown in Fig. 6.4 and Fig. 6.5, respectively. The total energy of the system is also shown in Fig. 6.6 which indicates that system is reaching to the zero-energy state asymptotically. From all the responses it can be seen that static dissipative controller exhibits asymptotic stability for the class of systems under consideration.

Since the synthesis procedure for DDC for nonlinear systems is not yet available, and the method of trial and error is also very cumbersome (unlike SDC) to obtain the controller parameters, an example is used where design of DDC is based on the locally linearized models of the nonlinear system. The advantage of using DDC is that even though the plant model used to design the controller was linear, the controller provides asymptotic stability to the complete nonlinear system as long as the constraints on the controller design variables are satisfied. The next section gives the example which illustrates this approach [44]. The example also illustrates the suitability of DDC in the integrated design framework.

6.2 Application of DDC to Integrated Design

As an example of the application of dynamic dissipative controllers to multibody nonlinear space system, an integrated design problem is considered. The generic prototype considered is as shown in Fig. 6.7.

The system under consideration, illustrated in Fig. 6.7, is intended to represent a simplified planar version of a flexible spacecraft with two articulated appendages. It has an articulated, flexible link placed at one end and an antenna at the other end. Typically, the antenna has stringent pointing requirements while the articulated link is slewed for scanning or servicing purposes. Actuators are located

at points A_1, A_2, and A_3. The main truss (platform) attitude is maintained using torque actuator at point A_2. Two articulated members are attached to the main platform via hinged joints with torque actuators at points A_1 and A_3. The member at point A_1 is representative of an "antenna-like" member with precision pointing requirements, while the member attached at A_3 represents a slewing component such as a manipulator arm. For the present study, the actuators at A_1 and A_2 are used to maintain constant platform attitude and antenna position, respectively, while the actuator at A_3 is used for slewing motion of the manipulator arm. All members are flexible, and for simplicity, each is modeled as a solid rod. The diameters of these rods are the structural design parameters in the optimization.

6.2.1 Integrated Design Approach

For pointing control it is generally acceptable to use a linearized model for the controller design. For a problem with linear vibratory motion, the linearization is performed relative to some prescribed nominal operating point. The resulting linearized model, and in-turn the controller design, depend upon the particular operating point. Since, in the case of problems with articulated appendages, there is no well defined operating point, any controller design must satisfy the performance requirements everywhere in the configuration space. The integrated design problem is that of designing the controller concurrently with the structure to minimize a performance function consistent with a set of prescribed constraints. The conventional method is to design the structure first and then design the controller based on the fixed structural design to satisfy a performance criterion. The design obtained through this sequential process is control optimized but not optimal in an overall integrated system sense. The integrated design procedure utilizes simultaneous design of the structure and controller for optimal interaction.

The prototype structure used for the integrated design problem is made up of three sections. Each section is modeled as a solid rod. The diameter of each rod is treated as a structural design parameter. The objective is to achieve a design which is closed-loop stable throughout the entire configuration space of the articulated member and at the same time satisfies the constraints on the structural design variables. The constraints on the structural design variables are of the type $d_i \leq d_{max}$, where d_i is the diameter of the i-th structural member. An additional requirement of minimizing control power is also added to the objective function. A schematic of a design procedure is shown in 6.8. For the purposes of this example, only the first three flexible modes of each member are considered in the design. The controller design is carried out in the presence of actuator noise and noise in the position and rate sensors which are collocated with the actuators. The performance function to be minimized is

$$J = \lim_{T\to\infty} \frac{1}{T}\mathcal{E}\int_0^T (y_p^T Q_p y_p + y_r^T Q_r y_r + u^T R u)dt \tag{6.1}$$

where Q_p, Q_r, and R are symmetric and positive definite weighting matrices, and $\mathcal{E}$ is an expectation operator. A dynamic dissipative controller consisting of three second-order blocks as in Eq. 3.22 is next designed. Using the transformation of Theorem 3.3 with $L = [\gamma_i, \delta_i]^T$ for $C_i(s)$, each $C_i(s)$ can be realized as a strictly proper controller:

$$\dot{\overline{x}}_{ci} = \begin{bmatrix} 0 & 1 \\ -\alpha_{0i} & -\alpha_{1i} \end{bmatrix} \overline{x}_{ci} + \begin{bmatrix} \delta_i & \gamma_i \\ \beta_{0i}\gamma_i + \beta_{1i}\delta_i & \delta_i \end{bmatrix} \begin{bmatrix} y_{pi} + w_{pi} \\ y_{ri} + w_{ri} \end{bmatrix}$$

$$u = (u_1, u_2, u_3)^T; \qquad u_i = (\beta_{0i} - \alpha_{0i})\overline{x}_{ci}$$

There are 18 control design variables ($\alpha_{0i}, \alpha_{1i}, \beta_{0i}, \beta_{1i}, \gamma_i, \delta_i$, $i = 1,2,3$) for the sixth-order controller. To ensure that the controller is dissipative, the constraints to be satisfied by the control design variables are 3.24, and that $\alpha_{0i}, \alpha_{1i}, \beta_{0i}, \beta_{1i}$ must be positive for $i = 1,2,3$. Also, due to the strictly proper realization of the controller the constraints on k_is in 3.22 are now transformed into the following constraints.

$$(\alpha_{1i} - \beta_{1i})\delta_i + (\alpha_{0i} - \beta_{0i})\gamma_i > 0$$

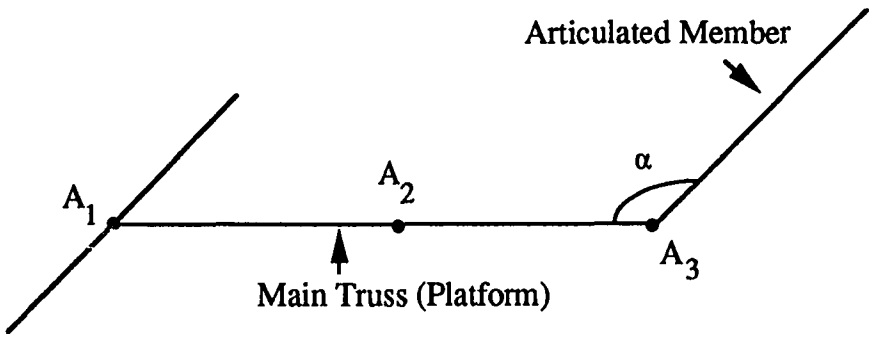

Fig. 6.7 Schematic of a flexible spacecraft with articulated member

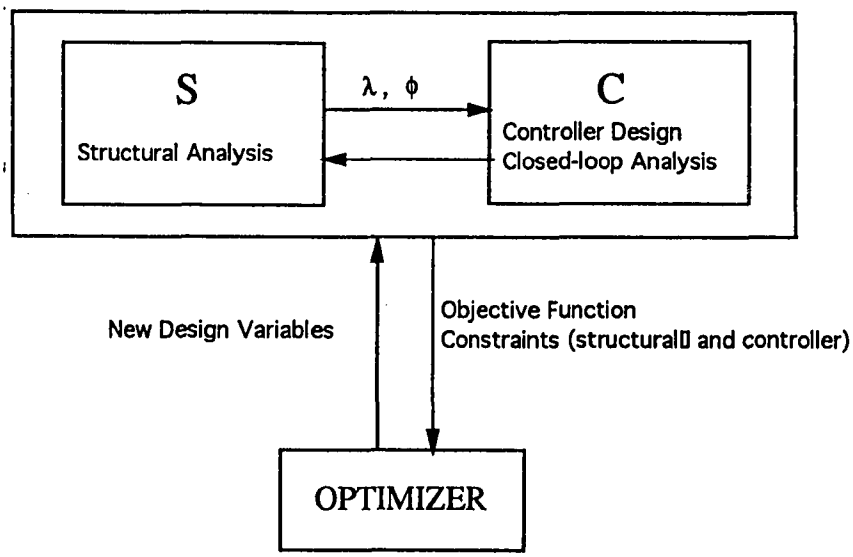

Fig. 6.8 Schematic of design procedure

where $i = 1, 2, 3$. The performance function J can be computed by solving the steady-state covariance equation for the closed-loop state equation of the plant and controller.

A dynamic dissipative controller (DDC) was designed by performing numerical minimization of the performance function with respect to the 18 control design variables and 3 structural design variables. The DDC has guaranteed stability in the presence of higher modes as well as parametric uncertainties. In order to ensure a reasonable transient response, additional constraints were imposed that the real parts of the closed-loop eigenvalues be no greater than -0.05. The optimization routine used is ADS (A fortran program for Automated Design Synthesis) [45]. The goal of this example problem is to produce an integrated design which satisfies the constraints and minimizes a performance index throughout the configuration space. To this end, the configuration space is partitioned into N_s segments, the performance index J_i (where J_i is given by Eq. 6.1 for i-th segment) is evaluated for each segment and the sum of these segment indices is defined as the global performance index

$$J_G = \sum_{i=1}^{N_s} J_i \tag{6.2}$$

It is this global performance index which is minimized in the design optimization. The configuration space is divided into $N_s = 24$ segments representing 0.131 radian increments of the joint angle α over the range $0 \leq \alpha \leq \pi$ radians. In sum, there are 25 configurations, and for each configuration there are 12 closed-loop eigenvalue constraints to be satisfied. Also, there are nine constraints on the control design variables. Therefore, the total number of constraints to be satisfied for each iteration of the optimization run is 309.

To reduce computational load, eigenvalues and eigenvectors are computed for only four baseline configurations and at intermediate configurations Taylor series approximations are used. The fourth-order approximation has been used for this example. The details of the first- and higher-order derivatives of the eigenvectors

with respect to the change in the orientation of the appendage have been derived in [46]. The eigensystem analysis was done for the four baseline configurations. For all other configurations the eigensystem approximation scheme was used.

6.2.2 Results

The design of the prototype structure obtained satisfies dimensional requirements for the structure and yields a guaranteed stable controller for all possible operating configurations. The history of the global performance index J_G is plotted in 6.9.

After a few initial oscillations, the value steadily decreases to the convergence value of 2.497. The initial oscillations are due to the fact that the optimization algorithm first tries to satisfy constraints and then minimizes the performance index. Table 1 gives the initial and final design parameter values resulting from the global optimization and also from two local optimizations using baseline configurations, $\alpha = \pi/8$ and $\alpha = \pi/2$. The final values of performance indices are also given. In the globally optimized case the value of J given is an average value (where average value is given by $\frac{J_G}{N_s}$). Table 6.1 also gives the total number of violated constraints for the entire configuration space.

Note that the designs obtained differ in each of the three cases considered. The designs based on fixed operating points violate the design constraints at some other configurations. The global optimization gives some minimum level of guaranteed closed-loop stability. Because the controller is dissipative, stability is guaranteed even in the locally optimized cases, however, the degree of stability cannot be assured for all configurations. The final value of J obtained through global optimization is larger than the one obtained through locally optimized designs, which is to be expected.

Design Variable Number	Initial Design Variables	Design Variables at Globally Optimal Design	Design Variables at Locally ($\alpha=\pi/3$) Optimal Design
Control Variables			
α_{01}	62.741	80.000	18.291
α_{11}	4.0718	11.311	10.590
α_{02}	3.6209	0.73088	1.4234
α_{12}	3.0380	6.8356	3.3611
α_{03}	1.3871	1.4411	1.5688
α_{13}	1.7177	7.2483	3.8302
β_{01}	0.42742	0.95401	0.9391
β_{11}	3.9023	10.809	10.109
β_{02}	0.0100	0.018721	0.0754
β_{12}	1.2590	0.27666	0.5280
β_{03}	0.16199	0.04235	0.08971
β_{13}	0.78550	0.39692	0.5604
δ_1	36.4140	80.000	65.021
δ_2	80.0000	78.937	73.811
δ_3	35.8080	40.619	37.644
γ_1	70.0000	79.9937	69.967
γ_2	18.331	79.859	30.770
γ_3	6.9030	31.763	14.556
Structural Variables			
r1	0.12593	0.074432	0.0662
r2	0.056056	0.059515	0.0552
r3	0.046352	0.076891	0.0675

Table 6.1 Comparison of design variables

6.3 Hoop/Column Antenna Example

This section illustrates another numerical example on the application of dynamic dissipative controller to the 122 meter diameter hoop-column antenna concept shown in Fig. 6.10.

The antenna consists of a deployable mast attached to a deployable hoop by cables held in tension. The antenna has many significant elastic modes which include mast bending, torsion, and reflective surface distortion. The objective is to control the attitude (including rigid and elastic components) at a certain point on the mast in the presence of actuator noise and noise in the attitude and rate sensors, which are collocated with three torque actuators, one for each axis. Table 6.2 shows the natural frequencies for the first 10 elastic modes. The open loop damping ratio is assumed to be 1 percent. A 12th order LQG controller, based on a design model consisting of the three rotational rigid modes and the first three elastic modes, was first designed to minimize:

$$J = \lim_{T\to\infty} \frac{1}{T}\mathcal{E}\int_0^T (y_p^T Q_p y_p + y_r^T Q_r y_r + u^T R u)dt \tag{6.3}$$

with $Q = 4\times 10^8 I_3$; $Q_r = 10^8 I_3$; $R = diag(0.1, 0.1, 1)$. The actuator noise covariance intensity was: $0.1 I_3$ (ft-lb) and the attitude and rate sensor noise covariance intensity was 10^{-10} diag (0.25, 0.25, 2.5) [rad/sec and $(rad/sec)^2$ respectively]. The optimal value of J was 0.6036, and the closed-loop eigenvalues for the design model and the 12th-order controller are shown in Table 6.3. A dynamic dissipative controller consisting of three second-order blocks as in Eq. 3.22 was next designed. Using the transformation of Theorem 3.3 with $L = [\gamma_i, \delta_i]^T$ for $K_i(s)$, each $K_i(s)$ can be realized as a strictly proper controller:

$$\dot{\overline{x}}_{ki} = \begin{bmatrix} 0 & 1 \\ -\alpha_{0i} & -\alpha_{1i} \end{bmatrix} \overline{x}_{ki} + \begin{bmatrix} \delta_i & \gamma_i \\ \beta_{0i}\gamma_i + \beta_{1i}\delta_i & \delta_i \end{bmatrix} \begin{bmatrix} y_{pi} + w_{pi} \\ y_{ri} + w_{ri} \end{bmatrix}$$

$$u = (u_1, u_2, u_3)^T; \qquad u_i = (\beta_{0i} - \alpha_{0i})\overline{x}_{ki}$$

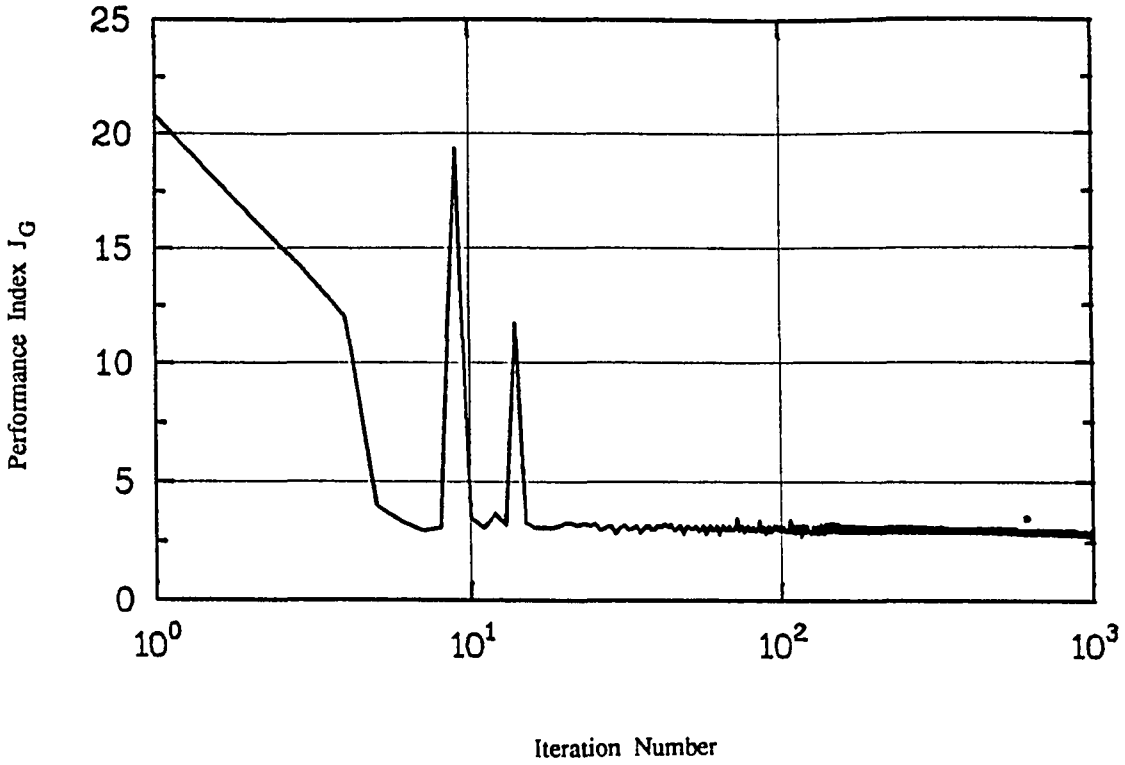

Fig. 6.9 Convergence history of global performance index

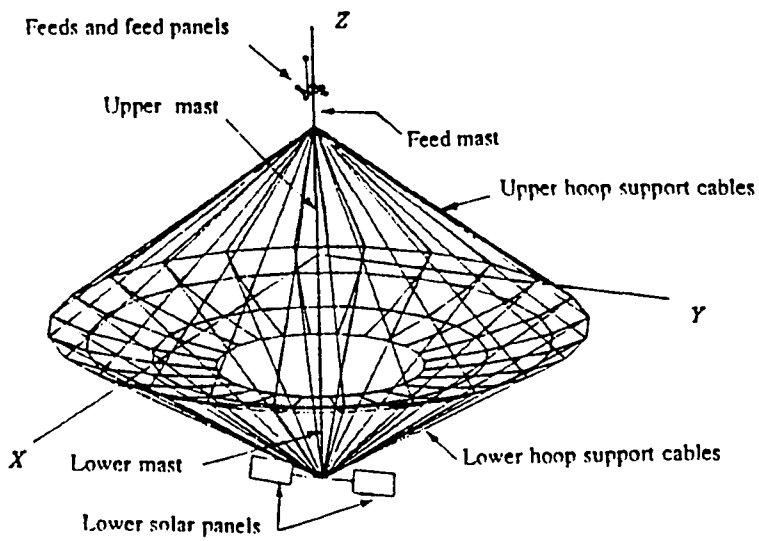

Fig. 6.10 Hoop/column antenna concept

0.75
1.35
1.70
3.18
4.53
5.59
5.78
6.84
7.40
8.78

Table 6.2 First 10 natural frequencies

-0.0035 ± 0.0194i
-0.0183 ± 0.0458i
-0.0160 ± 0.0502i
-0.3419 ± 0.5913i
-0.7179 ± 0.6428i
-0.8479 ± 0.5653i
-0.6482 ± 1.6451i
-0.4536 ± 2.1473i
-0.3764 ± 2.5522i

Table 6.3 Closed-loop eigenvalues for dynamic dissipative controller

The constraints to be satisfied are Eq. 3.24, and that $\alpha_{0i}, \alpha_{1i}, \beta_{0i}, \beta_{1i}$ are positive (i=1,2,3). Thus there are 18 design variables for this sixth-order compensater. The performance function in Eq. 6.3 can be computed by solving the steady-state covariance equation for the closed-loop state equation for the plant and the controller. A dynamic dissipative controller (DDC) was designed by performing numerical minimization of the performance function with respect to the 18 design variables. In order to ensure a reasonable transient response, an additional constraint is imposed, that the real parts of the closed-loop eigenvalues be not greater than -0.0035.

6.3.1 Results

Table 6.3 shows the resulting closed-loop eigenvalues. Although the value of J for the DDC was 1.2674 (about twice that for the LQG controller), the closed-loop eigenvalues indicate good performance. Furthermore, the LQG controller, which was based on the first six modes, caused instability when higher modes were included in the "evaluation" model, whereas the DDC has guaranteed stability in the presence of higher modes as well as parametric uncertainties.

Chapter 7

CONCLUSIONS AND FUTURE RESEARCH

7.1 Introduction

In this chapter, the principal results of this dissertation are summarized. Some conclusions about the stability results for static and dynamic dissipative compensators are presented and their significance is given. The chapter concludes with the suggestions for the future work which needs to be done in the related area.

7.2 Comments on Dynamic Modeling

The derivation of the dynamical equations of motion, given in chapter 2, is very general, i.e., any open-chained multibody, nonlinear, flexible system can be modeled by following the same methodology. Although the derivation of potential energy expression assumed that the system potential energy has contribution only from the elastic motion, any other form of potential energy can also be added in a similar manner. There are no specific assumptions regarding the geometrical aspects of the members. The flexibility is incorporated by using assumed modes method, however, any other technique for modeling flexibility can also be incorporated.

In summary, the mathematical model has been developed in a very compact form and is applicable to a wide class of multibody systems.

7.3 Stability With SDC

In chapter 4, it is proved that, nonlinear, multibody, flexible space structures exhibit global asymptotic stability under static dissipative control. The stability was shown to be robust not only to the modeling errors and parametric uncertainties, but also to a wide class of nonlinearities in the actuators and sensors. This result has a significant practical value since the mathematical models of the system usually have substantial inaccuracies, and the actuation and sensing devices available are not perfect. In other words, under certain conditions, with static dissipative controller, one can reposition any articulated payload on the space structure with guaranteed stability, even with imperfect actuators and sensors, as long as the conditions of the theorem are satisfied. It is also shown that in the case of deadzone type actuator nonlinearity, although the system trajectories do not go the equilibrium state asymptotically, they remain bounded in a compact region in the neighborhood of equilibrium point. This result is also very important since the deadzone type nonlinearities are very common and the controller design should at least assure that the system trajectories do not go unbounded. The numerical example given in chapter 6 validates some of the results.

7.4 Stability With DDC

The stability results obtained in chapter 4 for static dissipative controllers were extended to a more versatile class of controllers called dynamic dissipative controllers. These controllers are basically linear dynamic controllers satisfying certain dissipativity constraints. The result, that the dynamic dissipative controller can provide asymptotic stability to a nonlinear, multibody system, has significant practical value. The advantage of using dynamic dissipative controllers over the static dissipative type

is that the control designer has more design freedom which can be used for performance enhancement. For linear systems, these controllers are shown to give either equally good or better performance [33] than any other controller. In the case of nonlinear systems, however, other control techniques, such as, LQG, LQG/LTR, H_∞, μ-synthesis, etc., are not applicable (at least till now) to these systems and therefore, at present, the dissipative compensators seem to be the only potential candidates for nonlinear systems. In view of this, the theoretical developments done in chapters 4 and 5 are very instrumental in the control of nonlinear, multibody systems. The next section gives further enhancements that are needed to be done in this area and possible avenues that can be taken.

7.5 Future Research

The work presented in this dissertation suggests several problems for future investigation.

The most important one being the *synthesis* methods for both static and dynamic dissipative controllers. The synthesis of dynamic disspative compensators is very difficult even in the case of linear systems. In the case of linear systems, the performance function is well-defined and some systematic design procedure seems possible. However, in the case of nonlinear systems there is no systematic procedure known to design the controller. In view of this it seems that the synthesis of dissipative controllers for nonlinear systems is a challenging problem and offers a good potential for future research. Apart from synthesis procedure, some more enhancements are needed to the robust stability results to incorporate: i) certain imperfections in the collocation of actuators/sensors, ii) actuator dynamics in the case of dynamic dissipative controllers.

Another area for research is the use of nonlinear controllers in the dissipative framework. The theoretical development done in the area of passivity-based

controllers could be extended to include nonlinear controllers. Although it seems to be a very difficult task at present, it has a good potential for research.

In the case of spacecraft with articulated payloads, in particular, the robotic manipulators, some manipulator tasks may require tracking of certain trajectory, which is another potential problem for investigation. For the rigid robots this problem has been addressed by many researchers and continued research is being done. In the case of flexible manipulators, however, this problem is still not solved.

There are several other interesting topics, such as combined active and passive control using passive damping techniques, neural network controllers, etc., that are worthy of investigation.

REFERENCES

[1] Desoer, C. A., and Vidyasagar, M.: *Feedback Systems: Input-Output Properties.* Academic Press, Inc., New York, 1975.

[2] Popov, V. M.: *Hyperstability of Control Systems.* Springer-Velag, Berlin, 1973, pp. 118-138.

[3] Joshi, S. M.: *Control of Large Flexible Space Structures.* Berlin Springer-Verlag, 1989 (Vol. 131, Lecture Notes in Control and Information Sciences).

[4] Takegaki, M., and Arimoto, S.: A New Feedback Method for Dynamic Control of Manipulators. *ASME Journal of Dynamic Systems, Measurement and Control*, Vol. 102, June 1981.

[5] Koditschek, D. E.: Natural Control of Robot Arms. *Proc. 1984, IEEE Conference on Decision and Control*, Las Vegas, Nevada., pp. 733-735.

[6] Arimoto, S., and Miyazaki, F.: Stability and Robustness of PD Feedback Control With Gravity Compensation for Robot Manipulator. *ASME Winter Meeting*, Anaheim, California, December 1986, pp. 67-72.

[7] Vidyasagar, M.: *Nonlinear Systems Analysis*, 2nd ed., Englewood Cliffs, New Jersy, Prentice Hall, 1993.

[8] Paden, B., and Panja, R.: Globally Asymptotically Stable PD+ Controller for Robot Manipulators.*Int. Journal of Control*, 1988, Vol. 47, No. 6, pp 1697-1712.

[9] Wen, J. T., and Bayard, D. S.: A New Class of Control Laws for Robotic Manipulator. *Int. Journal of Control*, 1988, Vol. 47, No. 5, pp. 1361-1385.

[10] Paden, B., Riedle, B., and Bayo, E.: Exponentially Stable Tracking Control for Multi-Joint Flexible-Link Manipulators. *Proc. 1990, American Control Conference*, San Diego, California, May 23-25, 1990, pp. 680-684.

[11] Juang, J.-N., Wu, S.-C., Phan, M., and Longman, R. W.: Passive Dynamic Controllers for Nonlinear Mechanical Systems. NASA Technical Memorandum, TM 104047, March 1991.

[12] Willems, J., C.:Dissipative Dynamical Systems-Part I:General Theory, *Arch. Rational Mechanics and Analysis*, Vol. 45, 1972, pp. 321-351.

[13] Willems, J., C.:Dissipative Dynamical Systems-Part II:Linear Systems with Quadratic Supply Rates, *Arch. Rational Mechanics and Analysis*, Vol. 45, 1972, pp. 352-393.

[14] Benhabib, R. J., Iwens, R. P., and Jackson, R. L.: Stability of Large Space Structure Control Systems Using Positivity Concepts. *J. Guidance and Control*, Vol. 4, No.5, Sept.-Oct. 1981, pp. 487-494.

[15] Joshi, S. M., Maghami P. G., and Kelkar A. G.: Dynamic Dissipative Compensator Design for Large Space Structures. *AIAA Guidance, Navigation, and Control Conference*, New Orleans, Louisiana. August 12-14, 1991, paper no. AIAA 91-2650.

[16] Zames, G.: On the Input-Output Stability of Time-Varying Nonlinear Feedback Systems-Part I: Conditions derived using concepts of loop gain, conicity, and positivity, *IEEE Transactions on Automatic Control*, Vol. 11, 1966, pp. 228-238.

[17] Vidyasagar, M.: *Input-Output Analysis of Large-Scale Interconnected Systems*, Berlin, Springer-Verlag, 1981 (Vol. 29, Lecture Notes in Control and Information Sciences).

[18] Hill, D., and Moylan, P.: The stability of nonlinear dissipative systems, *IEEE Transactions on Automatic Control*, Vol. 21, 1976, pp. 708-711.

[19] Hill, D., and Moylan, P.: Stability results for nonlinear feedback systems, *Automatica*, Vol. 13, 1977, pp. 377-382.

[20] Hill, D., and Moylan, P.: Dissipative dynamical systems: Basic input-output and state properties, *J. Franklin Inst.*, Vol. 309, 1980, pp. 327-357.

[21] Hill, D., and Moylan, P.:Connections between finite gain and asymptotic stability, *IEEE Transactions on Automatic Control*, Vol. 25, 1980, pp. 931-936.

[22] Kwakernaak, H. and Sivan, R.:*Linear Optimal Control Systems*, New York, Wiley, 1972.

[23] Anderson, B. D. O. and Moore, J. B.:*Linear Optimal Control.* Englewood Cliffs, N. J., Prentice Hall, 1972.

[24] Bryson, A. E. Jr. and Ho, Y-C.:*Applied Optimal Control*, John Wiley and Sons, N.Y., 1975.

[25] Doyle, J. C.: Guaranteed Margins for LQG Controllers, *IEEE Transactions on Automatic Control*, Vol. AC-26, pp. 756-757, 1978.

[26] Doyle, J. C. and Stein, G.: Robustness with Observers, *IEEE Transactions on Automatic Control*, Vol. AC-24, pp. 607-611, 1979.

[27] Doyle, J. C. and Stein, G.: Multivariable Feedback Design: Concepts for a Classical/Modern Synthesis, *IEEE Transactions on Automatic Control*, Vol. AC-26, pp. 4-16, 1981.

[28] Stein, G.: LQG-based Multivariable Design: Frequency Domain Interpretations, *Multivariable Analysis and Design Techniques*, AGARD-LS-117, pp. 51-59, Sept. 1981.

[29] Maciejowski, J. M.: *Multivariable Feedback Design*, Addison-Wesley, 1990.

[30] Doyle, J. C., Glover, K., Khargonaker, P. P. and Francis, B. A.: State-Space Solutions to Standard H_2 and H_∞ Control Problems, *IEEE Transactions on Automatic Control*, Vol. 34, No. 8, pp. 831-847, Aug. 1989.

[31] Doyle, J. C.:Structured Uncertainty in Control System Design, *Proc. 24th IEEE Conf. on Decision and Control*, Fort Lauderdale, FL, pp.260-265, Dec. 1985.

[32] Glover, K. and Doyle, J. C.: State-space Formulae for All Stabilizing Controllers That Satisfy an H_∞ Norm Bound and Relation to Risk Sensitivity, *Systems and Control Letters*, Vol. 11, pp. 167-172, 1988.

[33] Lim, K. B., Maghami, P. G. and Joshi, S. M.: Comparison of Controller Designs for an Experimental Flexible Structure, *IEEE Control Systems*, pp. 108-118, June 1992.

[34] Anderson, B. D. O.: A System Theory Criterion for Positive Real Matrices, *SIAM J. on Control*, Vol. 5, No. 2, 1967, pp. 171-182.

[35] Lozano-Leal, R., and Joshi, S. M.: Strictly Positive Real Transfer Functions Revisited, *IEEE Transactions on Automatic Control*, Vol. 35, No. 11, Nov. 1990, pp. 1243-1245.

[36] McLaren, M. D., and Slater, G. L.: Robust Multivariable Control of Large Space Structures Using Positivity. *J.Guidance, Control and Dynamics*, Vol. 10, July-Aug. 1987, pp. 393-400.

[37] Slater, G. L., and McLaren, M. D.: Estimator Eigenvalue Placement in Positive Real Control. *J. Guidance, Control and Dynamics*, Vol. 13, No.1, Jun-Feb 1990, pp.168-175.

[38] Iwens, R. P., Benhabib, R. J., and Jackson, R. L.: A Unified Approach to the Design of Large Space Structure Control Systems, *Joint Automatic Control Conference*, San Francisco, CA, Aug. 13-15, 1980.

[39] Joshi, S. M., and Maghami P. G.: Dissipative Compensators for Flexible Spacecraft Control. *Proc. 1990 American Control Conference*, San Diego, CA, May 23-25, 1990.

[40] Willems, J., C.: *The Analysis of Feedback Systems*, Cambridge, MA: M.I.T. Press, 1971.

[41] Byrnes, C. I., Isidori, A., and Willems, J. C.: Passivity, Feedback Equivalence, and The Global Stabilization of Minimum Phase Nonlinear Systems, *IEEE Transactions on Automatic Control*, Vol. 36, 1991, pp. 1228-1240.

[42] Lasalle, J., and Lefschetz, S.: *Stability by Lyapunov's Direct Method* (Academic 1961).

[43] *DADS User's Manual*, Computer Aided Design Software, Inc. , Oakdale, Iowa 52319, July 1989.

[44] Kelkar, A. G., Koganti, G., Hou, G., Alberts, T. E. and Woodard, S.:'*CSI Design of Articulated Space Structures*,' Proc. AIAA/AAS Astrodynamics Conference, Hilton Head, SC, August 10-12, 1992, pp. 307-315.

[45] Vanderplaats, G. N.: *ADS - A Fortran Program For Automated Design Synthesis - Version 1.10.* NASA Contractor Report 177985.

[46] Koghanti, G.:*Linearized Dynamics of Space Structures with Articulated Appendages.* M.S. Thesis, Old Dominion University, 1991.

APPENDICES

APPENDIX A

Rotation Transformation Matrices

A 3×3 rotation matrix can be defined as a transformation matrix which operates on a vector in a three-dimensional euclidean space and maps its coordinates expressed in a rotated coordinate system to a reference coordinate system. Figure A.1 shows a reference coordinate system, $OXYZ$, and the rotated coordinate system(for example, a body fixed coordinate system), $OX''Y''Z''$. Let the orientation of $OX''Y''Z''$ be obtained by following sequence of rotations of $OXYZ$:

i) rotate by angle ϕ about OZ

ii) rotate by angle θ about new y axis

iii) rotate by angle ψ about new x axis

Then, corresponding rotation matrices are given by

$$R_{z,\phi} = \begin{bmatrix} C\phi & -S\phi & 0 \\ S\phi & C\phi & 0 \\ 0 & 0 & 1 \end{bmatrix}$$

$$R_{y,\theta} = \begin{bmatrix} C\theta & 0 & S\theta \\ 0 & 1 & 0 \\ -S\theta & 0 & C\theta \end{bmatrix}$$

$$R_{x,\psi} = \begin{bmatrix} 1 & 0 & 0 \\ 0 & C\psi & -S\psi \\ 0 & S\psi & C\psi \end{bmatrix}$$

and the composite rotation matrix is given by

$$R_{\phi,\theta,\psi} = R_{z,\phi} R_{y,\theta} R_{x,\psi}$$

$$= \begin{bmatrix} C\phi C\theta & C\phi S\theta S\psi - S\phi C\psi & C\phi S\theta C\psi + S\phi S\psi \\ S\phi S\theta & S\phi S\theta S\psi + C\phi C\psi & S\phi S\theta C\psi - C\phi S\psi \\ -S\theta & C\theta S\psi & C\theta C\psi \end{bmatrix} \quad \text{(A.1)}$$

A.1 Properties of Rotation Matrices

Several useful properties of rotation matrices are given below.

1. Each column vector of rotation matrix is a representation of the rotated axis unit vector expressed in terms of the axis unit vectors of the reference frame, and each row vector is a representation of the axis unit vector of the reference frame expressed in terms of the rotated axis unit vectors of the $OX''Y''Z''$ frame.

2. The determinant of a rotation matrix is +1 for a right-handed coordinate system and -1 for a left-handed coordinate system.

3. Since each row is a vector representation of orthonormal vectors, the inner product of each row with each other row equals zero. Same thing holds for columns.

4. The inverse of a rotation matrix is the transpose of the rotation matrix, i.e.

$$R^{-1} = R^T \qquad \text{and} \qquad RR^T = I_3$$

where, I_3 is a 3×3 identity matrix.

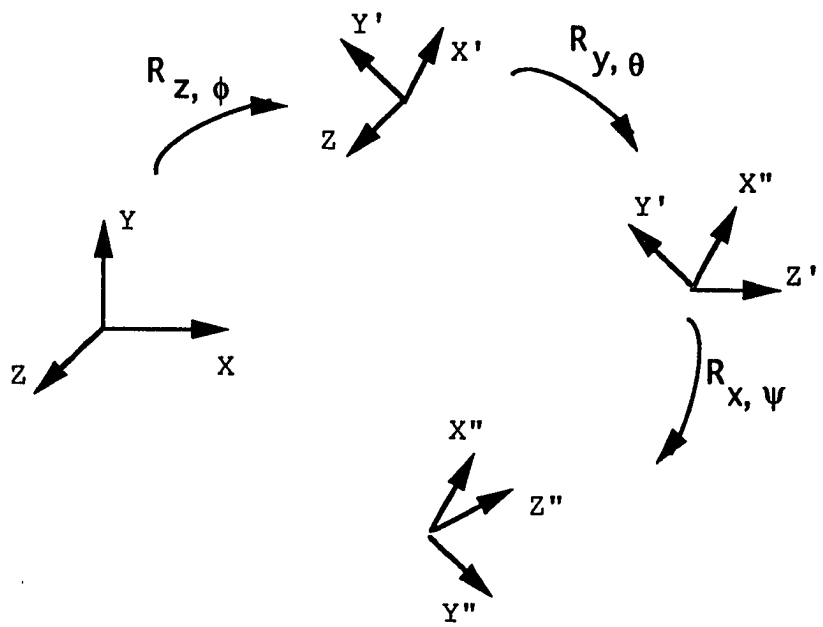

Fig. A.1 Reference and rotated coordinate frames.

APPENDIX B

NASTRAN Data Files for Arms

```
NASTRAN FILES=(DB01)
 ID CLASS IV GENERIC MODEL
 APP DISP
 SOL 3
 TIME 5000
 COMPILE DMAP=SOL3,SOUIN=MSCSOU
 ALTER 24
 OUTPUT2 GPL,BGPDT,,,//-1/21
 ALTER 26
 OUTPUT2 ECT,,,,//0/21
 ALTER 73
 OUTPUT4 MGG,,,,//-1/22
 OUTPUT4 ,,,,//-2/22
 OUTPUT2 OGPWG,,,,//0/21
$ ALTER 406
$ OUTPUT2 LAMA,,,,//-1/51
$ OUTPUT2,,,,//-9/51
 ALTER 416
```

```
 OUTPUT2 LAMA,,,,//0/21
 ALTER 439
$ OUTPUT2 OUGV1,,,,//-1/52
$ OUTPUT2,,,,//-9/52
 OUTPUT2 OUGV1,,,,//0/21
 OUTPUT2,,,,//-9/21
 ALTER 100
 OUTPUT4 KGG,,,,//-1/23
 OUTPUT4 ,,,,//-2/23
 ENDALTER
 CEND
 TITLE= GENERATION OF DADS FLEXIBLE INPUT
 SUBTITLE= ELEMENT : ARM 1
 OUTPUT
 LINES = 40
 SUBCASE 1
 METHOD = 1
 DISP = ALL
 SPC = 100
BEGIN BULK
PARAM   GRDPNT          0
MAT1,201,1.0E+07,,0.33,4.14E-04, 0.
EIGR,1,SINV,0.0,100.0,6,2,,,+eigr1
+eigr1,mass
SPC1, 100, 123456, 1
GRID, 1, , 0., 0., 0.
GRID, 2, , 5., 0., 0.
```

```
GRID, 3, ,10., 0., 0.
GRID, 4, ,15., 0., 0.
GRID, 5, ,20., 0., 0.
GRID, 6, ,25., 0., 0.
GRID, 7, ,30., 0., 0.
GRID, 8, ,35., 0., 0.
GRID, 9, ,40., 0., 0.
GRID,10, ,45., 0., 0.
GRID,11, ,50., 0., 0.
CBAR, 1, 102, 1, 2, 1., 0., 1.
CBAR, 2, 102, 2, 3, 1., 0., 1.
CBAR, 3, 102, 3, 4, 1., 0., 1.
CBAR, 4, 102, 4, 5, 1., 0., 1.
CBAR, 5, 102, 5, 6, 1., 0., 1.
CBAR, 6, 102, 6, 7, 1., 0., 1.
CBAR, 7, 102, 7, 8, 1., 0., 1.
CBAR, 8, 102, 8, 9, 1., 0., 1.
CBAR, 9, 102, 9,10, 1., 0., 1.
CBAR,10, 102,10,11, 1., 0., 1.
PBAR,102,201,0.786E+00,0.786E+00,1.57E+00,,0.
ENDDATA
```

APPENDIX C

NASTRAN Data File for Central Truss

```
NASTRAN FILES=(DB01)
 ID CLASS IV GENERIC MODEL
 APP DISP
 SOL 3
 TIME 5000
 COMPILE DMAP=SOL3,SOUIN=MSCSOU
 ALTER 24
 OUTPUT2 GPL,BGPDT,,,//-1/11
 ALTER 26
 OUTPUT2 ECT,,,,//0/11
 ALTER 73
 OUTPUT4 MGG,,,,//-1/12
 OUTPUT4 ,,,,//-2/12
 OUTPUT2 OGPWG,,,,//0/11
 ALTER 406
 OUTPUT2 LAMA,,,,//-1/51
```

```
 OUTPUT2,,,,//-9/51
 ALTER 416
 OUTPUT2 LAMA,,,,//0/11
 ALTER 439
 OUTPUT2 OUGV1,,,,//-1/52
 OUTPUT2,,,,//-9/52
 OUTPUT2 OUGV1,,,,//0/11
 OUTPUT2,,,,//-9/11
 ALTER 100
 OUTPUT4 KGG,,,,//-1/13
 OUTPUT4 ,,,,//-2/13
 ENDALTER
 CEND
 TITLE= GENERATION OF DADS FLEXIBLE INPUT
 SUBTITLE= ELEMENT : MAIN TRUSS
 OUTPUT
 LINES = 40
 SUBCASE 1
 METHOD = 1
 DISP = ALL
 SPC = 100
BEGIN BULK
PARAM   GRDPNT          0
MAT1,201,1.0E+07,,0.33,4.14E-04, 0.
EIGR,1,SINV,0.0,100.0,,32,,,+eigr1
+eigr1,mass
SUPORT,42,456
```

```
SPC1,100,123,46
GRID, 1, , 0., 0., 0.
GRID, 5, , 10., 0., 0.
GRID, 9, , 20., 0., 0.
GRID, 13, , 30., 0., 0.
GRID, 17, , 40., 0., 0.
GRID, 21, , 50., 0., 0.
GRID, 25, , 60., 0., 0.
GRID, 29, , 70., 0, 0.
GRID, 33, , 80., 0., 0.
GRID, 37, , 90., 0., 0.
GRID, 41, , 100., 0., 0.
GRID, 2, , 0., 10., 0.
GRID, 6, , 10., 10., 0.
GRID, 10, , 20., 10., 0.
GRID, 14, , 30., 10., 0.
GRID, 18, , 40., 10., 0.
GRID, 22, , 50., 10., 0.
GRID, 26, , 60., 10., 0.
GRID, 30, , 70., 10., 0.
GRID, 34, , 80., 10., 0.
GRID, 38, , 90., 10., 0.
GRID, 42, , 100., 10., 0.
GRID, 3, , 0.,10.,-10.
GRID, 7, , 10.,10.,-10.
GRID, 11, , 20.,10.,-10.
GRID, 15, , 30.,10.,-10.
```

```
GRID, 19, , 40.,10.,-10.
GRID, 23, , 50.,10.,-10.
GRID, 27, , 60.,10.,-10.
GRID, 31, , 70.,10.,-10.
GRID, 35, , 80.,10.,-10.
GRID, 39, , 90.,10.,-10.
GRID, 43, , 100.,10.,-10.
GRID, 4, , 0., 0., -10.
GRID, 8, , 10., 0., -10.
GRID, 12, , 20., 0., -10.
GRID, 16, , 30., 0., -10.
GRID, 20, , 40., 0., -10.
GRID, 24, , 50., 0., -10.
GRID, 28, , 60., 0., -10.
GRID, 32, , 70., 0., -10.
GRID, 36, , 80., 0., -10.
GRID, 40, , 90., 0., -10.
GRID, 44, , 100., 0., -10.
GRID, 45, , 100., 5., 0.
GRID, 46, , 50., 5., -5.
CBAR, 1, 101, 1, 2, 0., 1., 1.
CBAR, 2, 101, 2, 3, 0., 1., 1.
CBAR, 3, 101,3, 4, 0., 1., 1.
CBAR, 4, 101,4, 1, 0., 1., 1.
CBAR, 5, 101,5, 6, 0., 1., 1.
CBAR, 6, 101,6, 7, 0., 1., 1.
CBAR, 7, 101,7, 8, 0., 1., 1.
```

```
CBAR, 8, 101,8, 5, 0., 1., 1.
CBAR, 9, 101,9, 10, 0., 1., 1.
CBAR, 10, 101, 10, 11, 0., 1., 1.
CBAR, 11, 101, 11, 12, 0., 1., 1.
CBAR, 12, 101, 12, 9, 0., 1., 1.
CBAR, 13, 101, 13, 14, 0., 1., 1.
CBAR, 14, 101, 14, 15, 0., 1., 1.
CBAR, 15, 101, 15, 16, 0., 1., 1.
CBAR, 16, 101, 16, 13, 0., 1., 1.
CBAR, 17, 101, 17, 18, 0., 1., 1.
CBAR, 18, 101, 18, 19, 0., 1., 1.
CBAR, 19, 101, 19, 20, 0., 1., 1.
CBAR, 20, 101,20, 17, 0., 1., 1.
CBAR, 21, 101, 21, 22, 0., 1., 1.
CBAR, 22, 101,22, 23, 0., 1., 1.
CBAR, 23, 101,23, 24, 0., 1., 1.
CBAR, 24, 101,24, 21, 0., 1., 1.
CBAR, 25, 101,25, 26, 0., 1., 1.
CBAR, 26, 101,26, 27, 0., 1., 1.
CBAR, 27, 101,27, 28, 0., 1., 1.
CBAR, 28, 101,28, 25, 0., 1., 1.
CBAR, 29, 101,29, 30, 0., 1., 1.
CBAR, 30, 101,30, 31, 0., 1., 1.
CBAR, 31, 101, 31, 32, 0., 1., 1.
CBAR, 32, 101,32, 29, 0., 1., 1.
CBAR, 33, 101,33, 34, 0., 1., 1.
CBAR, 34, 101,34, 35, 0., 1., 1.
```

```
CBAR, 35, 101,35, 36, 0., 1., 1.
CBAR, 36, 101,36, 33, 0., 1., 1.
CBAR, 37, 101,37, 38, 0., 1., 1.
CBAR, 38, 101,38, 39, 0., 1., 1.
CBAR, 39, 101,39, 40, 0., 1., 1.
CBAR, 40, 101,40, 37, 0., 1., 1.
CBAR, 41, 101, 41, 45, 0., 1., 1.
CBAR, 42, 101,42, 43, 0., 1., 1.
CBAR, 43, 101,43, 44, 0., 1., 1.
CBAR, 44, 101,44, 41, 0., 1., 1.
CBAR, 45, 101,2, 6, 1., 1., 0.
CBAR, 46, 101,6,10, 1., 1., 0.
CBAR, 47, 101, 10, 14, 1., 1., 0.
CBAR, 48, 101, 14, 18, 1., 1., 0.
CBAR, 49, 101, 18, 22, 1., 1., 0.
CBAR, 50, 101,22, 26, 1., 1., 0.
CBAR, 51, 101, 26, 30, 1., 1., 0.
CBAR, 52, 101,30, 34, 1., 1., 0.
CBAR, 53, 101,34, 38, 1., 1., 0.
CBAR, 54, 101,38, 42, 1., 1., 0.
CBAR, 55, 101,3, 7, 1., 1., 0.
CBAR, 56, 101,7, 11, 1., 1., 0.
CBAR, 57, 101, 11, 15, 1., 1., 0.
CBAR, 58, 101, 15, 19, 1., 1., 0.
CBAR, 59, 101, 19, 23, 1., 1., 0.
CBAR, 60, 101,23, 27, 1., 1., 0.
CBAR, 61, 101, 27, 31, 1., 1., 0.
```

```
CBAR, 62, 101,31, 35, 1., 1., 0.
CBAR, 63, 101,35, 39, 1., 1., 0.
CBAR, 64, 101,39, 43, 1., 1., 0.
CBAR, 65, 101,4, 8, 1., 1., 0.
CBAR, 66, 101,8, 12, 1., 1., 0.
CBAR, 67, 101, 12, 16, 1., 1., 0.
CBAR, 68, 101, 16, 20, 1., 1., 0.
CBAR, 69, 101,20, 24, 1., 1., 0.
CBAR, 70, 101,24, 28, 1., 1., 0.
CBAR, 71, 101, 28, 32, 1., 1., 0.
CBAR, 72, 101,32, 36, 1., 1., 0.
CBAR, 73, 101,36, 40, 1., 1., 0.
CBAR, 74, 101,40, 44, 1., 1., 0.
CBAR, 75, 101, 1, 5, 1., 1., 0.
CBAR, 76, 101,5, 9, 1., 1., 0.
CBAR, 77, 101,9, 13, 1., 1., 0.
CBAR, 78, 101, 13, 17, 1., 1., 0.
CBAR, 79, 101, 17, 21, 1., 1., 0.
CBAR, 80, 101,21, 25, 1., 1., 0.
CBAR, 81, 101, 25, 29, 1., 1., 0.
CBAR, 82, 101,29, 33, 1., 1., 0.
CBAR, 83, 101,33, 37, 1., 1., 0.
CBAR, 84, 101,37, 41, 1., 1., 0.
CBAR, 85, 101,45, 42, 0., 1., 1.
CBAR, 86, 101,21, 46, 0., 0., 1.
CBAR, 87, 101,22, 46, 0., 0., 1.
CBAR, 88, 101,23, 46, 0., 0., 1.
```

```
CBAR, 89, 101,24, 46, 0., 0., 1.
$Battens
CBAR, 90, 101, 3, 6, 0., 0., 1.
CBAR, 91, 101, 6, 11,  0., 0., 1.
CBAR, 92, 101, 11, 14,  0., 0., 1.
CBAR, 93, 101, 14, 19,  0., 0., 1.
CBAR, 94, 101, 19, 22,  0., 0., 1.
CBAR, 95, 101, 22, 27,  0., 0., 1.
CBAR, 96, 101, 27, 30,  0., 0., 1.
CBAR, 97, 101, 30, 35,  0., 0., 1.
CBAR, 98, 101, 35, 38,  0., 0., 1.
CBAR, 99, 101, 38, 43,  0., 0., 1.
CBAR, 100, 101, 1, 8,  0., 0., 1.
CBAR, 101, 101, 8, 9,  0., 0., 1.
CBAR, 102, 101, 9, 16,  0., 0., 1.
CBAR, 103, 101, 16, 17,  0., 0., 1.
CBAR, 104, 101, 17, 24,  0., 0., 1.
CBAR, 105, 101, 24, 25,  0., 0., 1.
CBAR, 106, 101, 25, 32,  0., 0., 1.
CBAR, 107, 101, 32, 33,  0., 0., 1.
CBAR, 108, 101, 33, 40,  0., 0., 1.
CBAR, 109, 101, 40, 41,  0., 0., 1.
CBAR, 110, 101, 1, 6,  0., 1., 0.
CBAR, 111, 101, 6, 9,  0., 1., 0.
CBAR, 112, 101, 9, 14,  0., 1., 0.
CBAR, 113, 101, 14, 17,  0., 1., 0.
CBAR, 114, 101, 17, 22,  0., 1., 0.
```

```
CBAR, 115, 101, 22, 25,  0., 1., 0.
CBAR, 116, 101, 25, 30,  0., 1., 0.
CBAR, 117, 101, 30, 33,  0., 1., 0.
CBAR, 118, 101, 33, 38,  0., 1., 0.
CBAR, 119, 101, 38, 41,  0., 1., 0.
CBAR, 120, 101, 3, 8,  0., 1., 0.
CBAR, 121, 101, 8, 11,  0., 1., 0.
CBAR, 122, 101, 11, 16,  0., 1., 0.
CBAR, 123, 101, 16, 19,  0., 1., 0.
CBAR, 124, 101, 19, 24,  0., 1., 0.
CBAR, 125, 101, 24, 27,  0., 1., 0.
CBAR, 126, 101, 27, 32,  0., 1., 0.
CBAR, 127, 101, 32, 35,  0., 1., 0.
CBAR, 128, 101, 35, 40,  0., 1., 0.
CBAR, 129, 101, 40, 43,  0., 1., 0.
$Diagonals
CBAR, 130, 101, 1, 3,  0., 1., 0.
CBAR, 131, 101, 9, 11,  0., 1., 0.
CBAR, 132, 101, 17, 19,  0., 1., 0.
CBAR, 133, 101, 25, 27,  0., 1., 0.
CBAR, 134, 101, 33, 35,  0., 1., 0.
CBAR, 135, 101, 41, 43,  0., 1., 0.
CBAR, 136, 101, 6, 8,  0., 1., 0.
CBAR, 137, 101, 14, 16,  0., 1., 0.
CBAR, 138, 101, 30, 32,  0., 1., 0.
CBAR, 139, 101, 38, 40,  0., 1., 0.
$
```

```
$MPC, 100, 45, 1, 1.0, 46, 1, -1.0
$MPC, 100, 45, 2, 1.0, 46, 2, -1.0
$MPC, 100, 45, 3, 1.0, 46, 3, -1.0
$MPC, 100, 47, 1, 1.0, 48, 1, -1.0
$MPC, 100, 47, 2, 1.0, 48, 2, -1.0
$MPC, 100, 47, 3, 1.0, 48, 3, -1.0
PBAR,101,201,0.196E+00,4.9E-02,4.9E-02,,0.0
$PBAR,102,201,.7000000E+00,.0389929E-00,.0389929E-00,,.1520115E-01
ENDDATA
```

APPENDIX D

DADS Verbose File for the Model

```
ANALYSIS

CREATE SYSTEM.DATA
   UNITS                          := 'INCHES'
   ANALYSIS.TYPE                  := 'DYNAMIC'
   STARTING.TIME                  := '0.0'
   ENDING.TIME                    := '30.0'
   PRINT.INTERVAL                 := '0.05'
   GRAVITY.SEA.LEVEL              := '386.088'
   X.GRAVITY                      := '0.0'
   Y.GRAVITY                      := '0.0'
   Z.GRAVITY                      := '-1.0'
   SCALE.GRAVITY.COEF             := '0.0'
   MATRIX.OPERATIONS              := 'SPARSE'
   REDUNDANCY.CHECK               := 'TRUE'
   LU.TOL                         := '1.0D-12'
   ASSEMBLY.TOL                   := '2.0D-3'
   BYPASS.ASSEMBLY                := 'FALSE'
   OUTPUT.FILE                    := 'BOTH'
```

```
   REFERENCE.FRAME                 := 'LOCAL'
   DEBUG.FLAG                      := 'FALSE'
UP
CREATE DYNAMIC.DATA
   REACTION.FORCES                 := 'FALSE'
   FORCE.COORDINATES               := 'GLOBAL'
   PRINT.METHOD                    := 'INTERPOLATED'
   MAX.INT.STEP                    := '0.05'
   SOLUTION.TOL                    := '0.001'
   INTEGRATION.TOL                 := '0.0001'
   METHOD.INTEGRATION              := 'VARIABLE'
   PRINT.FREQ                      := '0'
UP
UP
FORCE
CREATE RSDA
   NAME                            := 'RSDA1'
   JOINT.NAME                      := 'REV1'
   ORIENTATION.ANGLE               := '0.0'
   SPRING.CONSTANT                 := '0.0'
   DAMPING.COEFFICIENT             := '0.0'
   ACTUATOR.TORQUE                 := '0.0'
   CURVE.SPRING                    := 'NONE'
   CURVE.DAMPER                    := 'NONE'
   CURVE.ACTUATOR                  := 'NONE'
   ANGULAR.UNITS                   := 'DEGREES'
   TYPE                            := 'BIDIRECTIONAL'
```

```
UP
CREATE RSDA
   NAME                          := 'RSDA2'
   JOINT.NAME                    := 'REV2'
   ORIENTATION.ANGLE             := '0.0'
   SPRING.CONSTANT               := '0.0'
   DAMPING.COEFFICIENT           := '0.0'
   ACTUATOR.TORQUE               := '0.0'
   CURVE.SPRING                  := 'NONE'
   CURVE.DAMPER                  := 'NONE'
   CURVE.ACTUATOR                := 'NONE'
   ANGULAR.UNITS                 := 'DEGREES'
   TYPE                          := 'BIDIRECTIONAL'
UP
UP
JOINTS
CREATE BRACKET.JOINT
   NAME                          := 'BRA1'
   BODY.1.NAME                   := 'PHOCG'
   BODY.2.NAME                   := 'PHASE0'
   P.ON.BODY.1                   := ( 0.0, 0.0, 0.0 )
   P.ON.BODY.2                   := ( 50.0, 5.0, -5.0 )
   Q.ON.BODY.1                   := ( 0.0, 0.0, 1.0 )
   Q.ON.BODY.2                   := ( 50.0, 5.0, -4.0 )
   R.ON.BODY.1                   := ( 1.0, 0.0, 0.0 )
   R.ON.BODY.2                   := ( 51.0, 5.0, -5.0 )
   NODE.1                        := '0'
```

```
   NODE.2                          := '46'
UP
CREATE BRACKET.JOINT
   NAME                            := 'BRA2'
   BODY.1.NAME                     := 'PHASE0'
   BODY.2.NAME                     := 'BASE'
   P.ON.BODY.1                     := ( 100.0, 5.0, 0.0 )
   P.ON.BODY.2                     := ( 0, 0, 0 )
   Q.ON.BODY.1                     := ( 100.0, 5.0, 1.0 )
   Q.ON.BODY.2                     := ( 0, 0, 1 )
   R.ON.BODY.1                     := ( 101.0, 5.0, 0.0 )
   R.ON.BODY.2                     := ( 1, 0, 0 )
   NODE.1                          := '45'
   NODE.2                          := '0'
UP
CREATE BRACKET.JOINT
   NAME                            := 'BRA3'
   BODY.1.NAME                     := 'ARM1BS'
   BODY.2.NAME                     := 'ARM1'
   P.ON.BODY.1                     := ( 0.0, 0.0, 0.0 )
   P.ON.BODY.2                     := ( 0, 0, 0.0 )
   Q.ON.BODY.1                     := ( 0.0, 0.0, 1.0 )
   Q.ON.BODY.2                     := ( 1.0, 0, 0.0 )
   R.ON.BODY.1                     := ( 1.0, 0.0, 0.0 )
   R.ON.BODY.2                     := ( 0, 0, -1.0 )
   NODE.1                          := '0'
   NODE.2                          := '1'
```

```
UP
CREATE BRACKET.JOINT
   NAME                          := 'BRA4'
   BODY.1.NAME                   := 'ARM1'
   BODY.2.NAME                   := 'ARM12'
   P.ON.BODY.1                   := ( 50.0, 0.0, 0.0 )
   P.ON.BODY.2                   := ( 0, 0, 0 )
   Q.ON.BODY.1                   := ( 51.0, 0.0, 0.0 )
   Q.ON.BODY.2                   := ( 0, 0, 1 )
   R.ON.BODY.1                   := ( 50.0, 0.0, -1.0 )
   R.ON.BODY.2                   := ( 1, 0, 0 )
   NODE.1                        := '11'
   NODE.2                        := '0'
UP
CREATE BRACKET.JOINT
   NAME                          := 'BRA5'
   BODY.1.NAME                   := 'ARM21'
   BODY.2.NAME                   := 'ARM2'
   P.ON.BODY.1                   := ( 0.0, 0.0, 0.0 )
   P.ON.BODY.2                   := ( 0, 0, 0 )
   Q.ON.BODY.1                   := ( 0.0, 0.0, 1.0 )
   Q.ON.BODY.2                   := ( 0, 0, -1 )
   R.ON.BODY.1                   := ( 1.0, 0.0, 0.0 )
   R.ON.BODY.2                   := ( -1, 0, 0 )
   NODE.1                        := '0'
   NODE.2                        := '1'
UP
```

```
CREATE REVOLUTE.JOINT
   NAME                          := 'REV1'
   BODY.1.NAME                   := 'BASE'
   BODY.2.NAME                   := 'ARM1BS'
   P.ON.BODY.1                   := ( 0.0, 0.0, 0.0 )
   P.ON.BODY.2                   := ( 0, 0, 0 )
   Q.ON.BODY.1                   := ( 0, 1, 0 )
   Q.ON.BODY.2                   := ( 0, -1, 0 )
   R.ON.BODY.1                   := ( 1.0, 0.0, 0.0 )
   R.ON.BODY.2                   := ( 1, 0, 0 )
   NODE.1                        := '0'
   NODE.2                        := '0'
UP
CREATE REVOLUTE.JOINT
   NAME                          := 'REV2'
   BODY.1.NAME                   := 'ARM12'
   BODY.2.NAME                   := 'ARM21'
   P.ON.BODY.1                   := ( 0, 0, 0 )
   P.ON.BODY.2                   := ( 0, 0, 0 )
   Q.ON.BODY.1                   := ( 0, 1, 0 )
   Q.ON.BODY.2                   := ( 0, -1, 0 )
   R.ON.BODY.1                   := ( 1, 0, 0 )
   R.ON.BODY.2                   := ( 1, 0, 0 )
   NODE.1                        := '0'
   NODE.2                        := '0'
UP
UP
```

```
CREATE BODY
   NAME                          := 'PHASE0'
   CENTER.OF.GRAVITY             := ( -50.0, -5.0, 5.0 )
   TYPE.ANGULAR.COORD            := 'EULER'
   ANGLE.1                       := '0.0'
   ANGLE.2                       := '0.0'
   ANGLE.3                       := '0.0'
   FIXED.TO.GROUND               := 'FALSE'
   MASS                          := '0.00697'
   INERTIA.XXL                   := '0.116'
   INERTIA.YYL                   := '5.87'
   INERTIA.ZZL                   := '5.87'
   INERTIA.XYL                   := '0.0'
   INERTIA.XZL                   := '0.0'
   INERTIA.YZL                   := '0.0'
   XG.FORCE                      := '0.0'
   YG.FORCE                      := '0.0'
   ZG.FORCE                      := '0.0'
   XL.TORQUE                     := '0.0'
   YL.TORQUE                     := '0.0'
   ZL.TORQUE                     := '0.0'
   CURVE.XGF                     := 'NONE'
   CURVE.YGF                     := 'NONE'
   CURVE.ZGF                     := 'NONE'
   CURVE.XLT                     := 'NONE'
   CURVE.YLT                     := 'NONE'
   CURVE.ZLT                     := 'NONE'
```

```
   SIGN.EO                          := 'POSITIVE'
   ANGULAR.UNITS                    := 'DEGREES'
   FLEXIBLE                         := 'TRUE'
   SUPERELEMENT                     := 'FALSE'
UP
CREATE BODY
   NAME                             := 'PHOCG'
   CENTER.OF.GRAVITY                := ( 0, 0, 0 )
   TYPE.ANGULAR.COORD               := 'EULER'
   ANGLE.1                          := '0.0'
   ANGLE.2                          := '0.0'
   ANGLE.3                          := '0.0'
   FIXED.TO.GROUND                  := 'FALSE'
   MASS                             := '0.0001'
   INERTIA.XXL                      := '0.0001'
   INERTIA.YYL                      := '0.0001'
   INERTIA.ZZL                      := '0.0001'
   INERTIA.XYL                      := '0.0'
   INERTIA.XZL                      := '0.0'
   INERTIA.YZL                      := '0.0'
   XG.FORCE                         := '0.0'
   YG.FORCE                         := '0.0'
   ZG.FORCE                         := '0.0'
   XL.TORQUE                        := '0.0'
   YL.TORQUE                        := '0.0'
   ZL.TORQUE                        := '0.0'
   CURVE.XGF                        := 'NONE'
```

```
   CURVE.YGF                    := 'NONE'
   CURVE.ZGF                    := 'NONE'
   CURVE.XLT                    := 'NONE'
   CURVE.YLT                    := 'NONE'
   CURVE.ZLT                    := 'NONE'
   SIGN.EO                      := 'POSITIVE'
   ANGULAR.UNITS                := 'DEGREES'
   FLEXIBLE                     := 'FALSE'
   SUPERELEMENT                 := 'FALSE'
UP
CREATE BODY
   NAME                         := 'ARM1'
   CENTER.OF.GRAVITY            := ( 50, 0, 5 )
   TYPE.ANGULAR.COORD           := 'EULER'
   ANGLE.1                      := '90'
   ANGLE.2                      := '-90'
   ANGLE.3                      := '-90'
   FIXED.TO.GROUND              := 'FALSE'
   MASS                         := '1.63E-02'
   INERTIA.XXL                  := '3.40'
   INERTIA.YYL                  := '3.40'
   INERTIA.ZZL                  := '0.815E-02'
   INERTIA.XYL                  := '0.0'
   INERTIA.XZL                  := '0.0'
   INERTIA.YZL                  := '0.0'
   XG.FORCE                     := '0.0'
   YG.FORCE                     := '0.0'
```

```
   ZG.FORCE                    := '0.0'
   XL.TORQUE                   := '0.0'
   YL.TORQUE                   := '0.0'
   ZL.TORQUE                   := '0.0'
   CURVE.XGF                   := 'NONE'
   CURVE.YGF                   := 'NONE'
   CURVE.ZGF                   := 'NONE'
   CURVE.XLT                   := 'NONE'
   CURVE.YLT                   := 'NONE'
   CURVE.ZLT                   := 'NONE'
   SIGN.E0                     := 'POSITIVE'
   ANGULAR.UNITS               := 'DEGREES'
   FLEXIBLE                    := 'TRUE'
   SUPERELEMENT                := 'FALSE'
UP
CREATE BODY
   NAME                        := 'ARM2'
   CENTER.OF.GRAVITY           := ( 50, 0, 55 )
   TYPE.ANGULAR.COORD          := 'EULER'
   ANGLE.1                     := '-180'
   ANGLE.2                     := '-180'
   ANGLE.3                     := '0'
   FIXED.TO.GROUND             := 'FALSE'
   MASS                        := '1.63E-02'
   INERTIA.XXL                 := '0.815E-02'
   INERTIA.YYL                 := '3.40'
   INERTIA.ZZL                 := '3.40'
```

```
   INERTIA.XYL                    := '0.0'
   INERTIA.XZL                    := '0.0'
   INERTIA.YZL                    := '0.0'
   XG.FORCE                       := '0.0'
   YG.FORCE                       := '0.0'
   ZG.FORCE                       := '0.0'
   XL.TORQUE                      := '0.0'
   YL.TORQUE                      := '0.0'
   ZL.TORQUE                      := '0.0'
   CURVE.XGF                      := 'NONE'
   CURVE.YGF                      := 'NONE'
   CURVE.ZGF                      := 'NONE'
   CURVE.XLT                      := 'NONE'
   CURVE.YLT                      := 'NONE'
   CURVE.ZLT                      := 'NONE'
   SIGN.E0                        := 'POSITIVE'
   ANGULAR.UNITS                  := 'DEGREES'
   FLEXIBLE                       := 'TRUE'
   SUPERELEMENT                   := 'FALSE'
UP
CREATE BODY
   NAME                           := 'BASE'
   CENTER.OF.GRAVITY              := ( 50, 0, 5 )
   TYPE.ANGULAR.COORD             := 'EULER'
   ANGLE.1                        := '0.0'
   ANGLE.2                        := '0.0'
   ANGLE.3                        := '0.0'
```

```
   FIXED.TO.GROUND                 := 'FALSE'
   MASS                            := '0.0001'
   INERTIA.XXL                     := '0.0001'
   INERTIA.YYL                     := '0.0001'
   INERTIA.ZZL                     := '0.0001'
   INERTIA.XYL                     := '0.0'
   INERTIA.XZL                     := '0.0'
   INERTIA.YZL                     := '0.0'
   XG.FORCE                        := '0.0'
   YG.FORCE                        := '0.0'
   ZG.FORCE                        := '0.0'
   XL.TORQUE                       := '0.0'
   YL.TORQUE                       := '0.0'
   ZL.TORQUE                       := '0.0'
   CURVE.XGF                       := 'NONE'
   CURVE.YGF                       := 'NONE'
   CURVE.ZGF                       := 'NONE'
   CURVE.XLT                       := 'NONE'
   CURVE.YLT                       := 'NONE'
   CURVE.ZLT                       := 'NONE'
   SIGN.EO                         := 'POSITIVE'
   ANGULAR.UNITS                   := 'DEGREES'
   FLEXIBLE                        := 'FALSE'
   SUPERELEMENT                    := 'FALSE'
UP
CREATE BODY
   NAME                            := 'ARM1BS'
```

```
CENTER.OF.GRAVITY          := ( 50, 0, 5 )
TYPE.ANGULAR.COORD         := 'EULER'
ANGLE.1                    := '0.0'
ANGLE.2                    := '0.0'
ANGLE.3                    := '0.0'
FIXED.TO.GROUND            := 'FALSE'
MASS                       := '0.0001'
INERTIA.XXL                := '0.0001'
INERTIA.YYL                := '0.0001'
INERTIA.ZZL                := '0.0001'
INERTIA.XYL                := '0.0'
INERTIA.XZL                := '0.0'
INERTIA.YZL                := '0.0'
XG.FORCE                   := '0.0'
YG.FORCE                   := '0.0'
ZG.FORCE                   := '0.0'
XL.TORQUE                  := '0.0'
YL.TORQUE                  := '0.0'
ZL.TORQUE                  := '0.0'
CURVE.XGF                  := 'NONE'
CURVE.YGF                  := 'NONE'
CURVE.ZGF                  := 'NONE'
CURVE.XLT                  := 'NONE'
CURVE.YLT                  := 'NONE'
CURVE.ZLT                  := 'NONE'
SIGN.EO                    := 'POSITIVE'
ANGULAR.UNITS              := 'DEGREES'
```

```
   FLEXIBLE                    := 'FALSE'
   SUPERELEMENT                := 'FALSE'
UP
CREATE BODY
   NAME                        := 'ARM12'
   CENTER.OF.GRAVITY           := ( 50, 0, 55 )
   TYPE.ANGULAR.COORD          := 'EULER'
   ANGLE.1                     := '0.0'
   ANGLE.2                     := '0.0'
   ANGLE.3                     := '0.0'
   FIXED.TO.GROUND             := 'FALSE'
   MASS                        := '0.0001'
   INERTIA.XXL                 := '0.0001'
   INERTIA.YYL                 := '0.0001'
   INERTIA.ZZL                 := '0.0001'
   INERTIA.XYL                 := '0.0'
   INERTIA.XZL                 := '0.0'
   INERTIA.YZL                 := '0.0'
   XG.FORCE                    := '0.0'
   YG.FORCE                    := '0.0'
   ZG.FORCE                    := '0.0'
   XL.TORQUE                   := '0.0'
   YL.TORQUE                   := '0.0'
   ZL.TORQUE                   := '0.0'
   CURVE.XGF                   := 'NONE'
   CURVE.YGF                   := 'NONE'
   CURVE.ZGF                   := 'NONE'
```

```
   CURVE.XLT                    := 'NONE'
   CURVE.YLT                    := 'NONE'
   CURVE.ZLT                    := 'NONE'
   SIGN.EO                      := 'POSITIVE'
   ANGULAR.UNITS                := 'DEGREES'
   FLEXIBLE                     := 'FALSE'
   SUPERELEMENT                 := 'FALSE'
UP
CREATE BODY
   NAME                         := 'ARM21'
   CENTER.OF.GRAVITY            := ( 50, 0, 55 )
   TYPE.ANGULAR.COORD           := 'EULER'
   ANGLE.1                      := '0.0'
   ANGLE.2                      := '0.0'
   ANGLE.3                      := '0.0'
   FIXED.TO.GROUND              := 'FALSE'
   MASS                         := '0.0001'
   INERTIA.XXL                  := '0.0001'
   INERTIA.YYL                  := '0.0001'
   INERTIA.ZZL                  := '0.0001'
   INERTIA.XYL                  := '0.0'
   INERTIA.XZL                  := '0.0'
   INERTIA.YZL                  := '0.0'
   XG.FORCE                     := '0.0'
   YG.FORCE                     := '0.0'
   ZG.FORCE                     := '0.0'
   XL.TORQUE                    := '0.0'
```

```
    YL.TORQUE                    := '0.0'
    ZL.TORQUE                    := '0.0'
    CURVE.XGF                    := 'NONE'
    CURVE.YGF                    := 'NONE'
    CURVE.ZGF                    := 'NONE'
    CURVE.XLT                    := 'NONE'
    CURVE.YLT                    := 'NONE'
    CURVE.ZLT                    := 'NONE'
    SIGN.EO                      := 'POSITIVE'
    ANGULAR.UNITS                := 'DEGREES'
    FLEXIBLE                     := 'FALSE'
    SUPERELEMENT                 := 'FALSE'
UP
CREATE FLEXIBLE
    NAME                         := 'PHASEOF'
    BODY.NAME                    := 'PHASEO'
    FILE.NAME                    := 'trussol_dads.dat'
    NUMBER.MODES                 := '2'
    FORCE.NODE                   := '0'
    XG.FORCE                     := '0.0'
    YG.FORCE                     := '0.0'
    ZG.FORCE                     := '0.0'
    RELATIVE.DAMPING             := '0.005'
UP
CREATE FLEXIBLE
    NAME                         := 'ARM1F'
    BODY.NAME                    := 'ARM1'
```

```
   FILE.NAME                    := 'arm1ol_dads.dat'
   NUMBER.MODES                 := '2'
   FORCE.NODE                   := '0'
   XG.FORCE                     := '0.0'
   YG.FORCE                     := '0.0'
   ZG.FORCE                     := '0.0'
   RELATIVE.DAMPING             := '0.005'
UP
CREATE FLEXIBLE
   NAME                         := 'ARM2F'
   BODY.NAME                    := 'ARM2'
   FILE.NAME                    := 'arm2ol_dads.dat'
   NUMBER.MODES                 := '2'
   FORCE.NODE                   := '0'
   XG.FORCE                     := '0.0'
   YG.FORCE                     := '0.0'
   ZG.FORCE                     := '0.0'
   RELATIVE.DAMPING             := '0.005'
UP
CREATE INITIAL.CONDITION
   NAME                         := 'INI1'
   BODY.1.NAME                  := 'PHOCG'
   BODY.2.NAME                  := 'NONE'
   ELEMENT.NAME                 := 'NONE'
   TYPE.INITIAL.COND            := 'X'
   INITIAL.VALUE                := '0'
   TIME.DERIVATIVE              := '0.0'
```

```
   OMEGA.Y                          := '0.0'
   OMEGA.Z                          := '0.0'
   P.ON.BODY.1                      := ( 0.0, 0.0, 0.0 )
   P.ON.BODY.2                      := ( 0.0, 0.0, 0.0 )
   EXTRA.COORD                      := '0'
   ANGULAR.UNITS                    := 'DEGREES'
UP
CREATE INITIAL.CONDITION
   NAME                             := 'INI2'
   BODY.1.NAME                      := 'PHOCG'
   BODY.2.NAME                      := 'NONE'
   ELEMENT.NAME                     := 'NONE'
   TYPE.INITIAL.COND                := 'Y'
   INITIAL.VALUE                    := '0'
   TIME.DERIVATIVE                  := '0.0'
   OMEGA.Y                          := '0.0'
   OMEGA.Z                          := '0.0'
   P.ON.BODY.1                      := ( 0.0, 0.0, 0.0 )
   P.ON.BODY.2                      := ( 0.0, 0.0, 0.0 )
   EXTRA.COORD                      := '0'
   ANGULAR.UNITS                    := 'DEGREES'
UP
CREATE INITIAL.CONDITION
   NAME                             := 'INI3'
   BODY.1.NAME                      := 'PHOCG'
   BODY.2.NAME                      := 'NONE'
   ELEMENT.NAME                     := 'NONE'
```

```
   TYPE.INITIAL.COND                := 'Z'
   INITIAL.VALUE                    := '0'
   TIME.DERIVATIVE                  := '0.0'
   OMEGA.Y                          := '0.0'
   OMEGA.Z                          := '0.0'
   P.ON.BODY.1                      := ( 0.0, 0.0, 0.0 )
   P.ON.BODY.2                      := ( 0.0, 0.0, 0.0 )
   EXTRA.COORD                      := '0'
   ANGULAR.UNITS                    := 'DEGREES'
UP
CREATE INITIAL.CONDITION
   NAME                             := 'INI4'
   BODY.1.NAME                      := 'PHOCG'
   BODY.2.NAME                      := 'NONE'
   ELEMENT.NAME                     := 'NONE'
   TYPE.INITIAL.COND                := 'ORIENTATION'
   INITIAL.VALUE                    := '0.0'
   TIME.DERIVATIVE                  := '0.0'
   OMEGA.Y                          := '0.0'
   OMEGA.Z                          := '0.0'
   P.ON.BODY.1                      := ( 0.0, 0.0, 0.0 )
   P.ON.BODY.2                      := ( 0.0, 0.0, 0.0 )
   EXTRA.COORD                      := '0'
   ANGULAR.UNITS                    := 'DEGREES'
UP
CREATE INITIAL.CONDITION
   NAME                             := 'INI5'
```

```
   BODY.1.NAME                    := 'NONE'
   BODY.2.NAME                    := 'NONE'
   ELEMENT.NAME                   := 'RSDA2'
   TYPE.INITIAL.COND              := 'REL.ANGLE'
   INITIAL.VALUE                  := '1.0'
   TIME.DERIVATIVE                := '0.0'
   OMEGA.Y                        := '0.0'
   OMEGA.Z                        := '0.0'
   P.ON.BODY.1                    := ( 0.0, 0.0, 0.0 )
   P.ON.BODY.2                    := ( 0.0, 0.0, 0.0 )
   EXTRA.COORD                    := '0'
   ANGULAR.UNITS                  := 'RADIANS'
UP
CREATE POINT.OF.INTEREST
   NAME                           := 'ARM1TIP'
   BODY.NAME                      := 'ARM1'
   P.ON.BODY                      := ( 50.0, 0.0, 0.0 )
   NODE                           := '11'
UP
CREATE POINT.OF.INTEREST
   NAME                           := 'ARM2TIP'
   BODY.NAME                      := 'ARM2'
   P.ON.BODY                      := ( 50.0, 0.0, 0.0 )
   NODE                           := '11'
UP
```